HHS Public Access

Author manuscript

Exp Neurol. Author manuscript; available in PMC 2020 November 01.

Published in final edited form as:

Exp Neurol. 2020 November ; 333: 113413. doi:10.1016/j.expneurol.2020.113413.

Preclinical evidence in support of repurposing sub-anesthetic ketamine as a treatment for L-DOPA-induced dyskinesia

Mitchell J. Bartlett[a,b], **Andrew J. Flores**[a,c], **Tony Ye**[a], **Saskia I. Smidt**[a], **Hannah K. Dollish**[d], **Jennifer A. Stancati**[e], **Drew C. Farrell**[f], **Kate L. Parent**[f], **Kristian P. Doyle**[a,g], **David G. Besselsen**[h], **Michael L. Heien**[f], **Stephen L. Cowen**[i], **Kathy Steece-Collier**[e], **Scott J. Sherman**[a], **Torsten Falk**[a,b,c,d,*]

[a]Department of Neurology, The University of Arizona, Tucson, AZ 85724, USA

[b]Department of Pharmacology, The University of Arizona, Tucson, AZ 85724, USA

[c]Graduate Interdisciplinary Program in Physiological Sciences, The University of Arizona, Tucson, AZ 85724, USA

[d]Graduate Interdisciplinary Program in Neuroscience, The University of Arizona, Tucson, AZ 85724, USA

[e]Department of Translational Neuroscience, Michigan State University, Grand Rapids, MI 49503, USA

[f]Department of Chemistry & Biochemistry, The University of Arizona, Tucson, AZ 85721, USA

[g]Department of Immunobiology, The University of Arizona, Tucson, AZ 85724, USA

[h]University Animal Care, The University of Arizona, Tucson, AZ 85724, USA

[i]Department of Psychology, The University of Arizona, Tucson, AZ 85724, USA

Abstract

Parkinson's disease (PD) is the second most common neurodegenerative disease. Pharmacotherapy with L-DOPA remains the gold-standard therapy for PD, but is often limited by the development of the common side effect of L-DOPA-induced dyskinesia (LID), which can become debilitating. The only effective treatment for disabling dyskinesia is surgical therapy (neuromodulation or lesioning), therefore effective pharmacological treatment of LID is a critical unmet need. Here, we show that sub-anesthetic doses of ketamine attenuate the development of LID in a rodent model, while also having acute anti-parkinsonian activity. The long-term anti-dyskinetic effect is mediated by brain-derived neurotrophic factor-release in the striatum, followed by activation of ERK1/2 and mTOR pathway signaling. This ultimately leads to

*Corresponding author at: Department of Neurology, The University of Arizona, Tucson, AZ 85724, USA. tfalk@u.arizona.edu (T. Falk).

Declaration of Competing Interest

SJS and TF have a pending patent application for the use of ketamine as a novel treatment for levodopa-induced dyskinesia associated with Parkinson's disease. The other authors have nothing to declare.

Appendix A. Supplementary data

Supplementary data to this article can be found online at https://doi.org/10.1016/j.expneurol.2020.113413.

morphological changes in dendritic spines on striatal medium spiny neurons that correlate with the behavioral effects, specifically a reduction in the density of mushroom spines, a dendritic spine phenotype that shows a high correlation with LID. These molecular and cellular changes match those occurring in hippocampus and cortex after effective sub-anesthetic ketamine treatment in preclinical models of depression, and point to common mechanisms underlying the therapeutic efficacy of ketamine for these two disorders. These preclinical mechanistic studies complement current ongoing clinical testing of sub-anesthetic ketamine for the treatment of LID by our group, and provide further evidence in support of repurposing ketamine to treat individuals with PD. Given its clinically proven therapeutic benefit for both treatment-resistant depression and several pain states, very common co-morbidities in PD, sub-anesthetic ketamine could provide multiple therapeutic benefits for PD in the future.

Keywords

Parkinson’s disease; Levodopa; Brain-derived neurotrophic factor; TrkB; mTOR; ERK1/2; Depression

1. Introduction

Parkinson’s disease (PD) is the second most common neurodegenerative disorder, affecting over 6 million people worldwide causing difficulties in many activities of daily living (Olanow et al., 2009; Schapira and Jenner, 2011). The cardinal motor symptoms of PD are largely due to the specific loss of the dopaminergic neurons in the substantia nigra (SN) pars compacta (Savitt et al., 2006). In addition, individuals with PD may experience a host of non-motor symptoms such as autonomic dysfunction, psychiatric (depression), cognitive and sensory symptoms (pain). Current symptomatic treatments are based primarily on dopamine (DA) replacement therapies with L-DOPA (levodopa) being the gold-standard; however, this treatment has long-term side effects which ultimately limits the use to control symptoms. The most severe side effect is the development of L-DOPA-induced dyskinesia (LID) (Huot et al., 2013), involuntary abnormal movements that, in some patients, can be as or even more debilitating than the cardinal symptoms (Marras and Turner, 2004). Approximately 80% of individuals with PD will develop LID within 10–12 years of L-DOPA treatment (Jankovic, 2005). Development of any adjunct therapy extending the time frame in which L-DOPA can be used without causing LID would be a major advancement for individuals living with PD.

Ketamine is a Food and Drug Administration (FDA)-approved drug with a known safety profile that has been used as an effective general anesthetic for over 50 years (Li and Vlisides, 2016). More recently, low-dose, sub-anesthetic ketamine infusions (0.1–0.3 mg/kg/h in human patients; 5–20 mg/kg in rodent models) have been shown to be an effective therapy for chronic pain states (Niesters et al., 2014), treatment-resistant depression (Andrade, 2017), and posttraumatic stress disorder (PTSD) symptoms (Feder et al., 2014). The reported therapeutic effects of ketamine in this group of disorders are neuroplastic in nature since the benefits last for weeks to months after the initial ketamine therapy. One commonality between migraine headaches (Rogawski, 2008), depression (Alamian et al., 2017), PTSD (Dunkley et al., 2014), PD (Savitt et al., 2006; Jenkinson and Brown,

2011), and LID (Herz et al., 2015) is that oscillatory electrical activity in the brain displays pathological hyper-synchrony. An additional link between these disorders is the development of maladaptive plastic changes at the synaptic, cellular and systems level that occur in many brain regions including the basal ganglia (BG), a brain region of particular interest in PD and LID. Since ketamine is known to alter oscillatory electrical brain activity in neural circuits, including motor circuits (Nicolás et al., 2011; Ye et al., 2018), we investigated the use of low-dose sub-anesthetic ketamine for the treatment of PD and LID. In a clinical case report, we previously showed that low-dose ketamine infusions had a long-term therapeutic effect (reduced dyskinesia, improved on-time, and reduced depression) in individuals with PD (Sherman et al., 2016). We also demonstrated the ability of 10-h sub-anesthetic ketamine treatment to reduce established LID in a 6-hydroxydopamine (6-OHDA) rat PD model (Bartlett et al., 2016), where significant suppression of LID lasted for several weeks. Taken together, these findings indicate an underlying neuroplastic mechanism.

In this current study, we investigated the therapeutic potential of low-dose ketamine to reduce the severity of LID expression and show initial findings relevant to the underlying mechanisms of ketamine's long-term effects. We employed two related but distinct *Experiments* utilizing a well-established rat model of LID (Cenci and Crossman, 2018). Rats were rendered unilaterally parkinsonian with the neurotoxin 6-OHDA and treated daily with L-DOPA to induce LID. In *Experiment 1,* we compared the effect of ketamine (which is a racemic mixture consisting of two enantiomers, *R*- and *S*-ketamine), to that of the enantiomer *R*-ketamine to attenuate the development of LID using a 10-h exposure paradigm. *R*-ketamine was tested because a recent preclinical study has indicated it could be antidepressive with a slightly reduced psychomimetic liability (Yang et al., 2015). In *Experiment 2* we tested for anti-parkinsonian activity of ketamine. To begin to understand the mechanisms involved in this effect, in *Experiment 3*, we examined whether blocking brain-derived neurotrophic factor (BDNF) signaling would inhibit the anti-dyskinetic action of ketamine using a similar paradigm.

2. Material and methods

2.1. Abbreviations

All abbreviations are summarized in Table 1

2.2. Animals

Adult male, Sprague-Dawley rats (225 g at arrival, Envigo RMC Inc., Indianapolis, IN), were housed two per cage throughout the study in a temperature and humidity-controlled room on a 12-h reverse light/dark cycle. Food and water were provided *ad libitum*. All animal studies were approved by the Institutional Animal Care and Use Committee at The University of Arizona, were performed in accordance with the NIH Guidelines for the Care and Use of Laboratory Animals, and the ARRIVE guidelines.

2.3. Unilateral 6-hydroxydopamine (6-OHDA) lesion

Rats (n = 110, 250–300 g at time of surgery) were pretreated (30-min prior to 6-OHDA administration) with 12.5 mg/kg desipramine hydrochloride in sterile 0.9% normal saline,

with 10% dimethyl sulfoxide (DMSO; Sigma-Aldrich, St. Louis, MO) to prevent loss of noradrenergic neurons. Anesthesia was administered by isoflurane (1.5–2.0%; VetOne, Boise, ID) mixed in a vaporizer (JD Medical, Phoenix, AZ) with 1.5 l of oxygen/min. 6-OHDA (5.0 μg/μl in sterile 0.9% normal saline with 0.02% ascorbic acid; Sigma-Aldrich) was administered (0.5 μl/min) using a microinjector (Stoelting Co., Wood Dale, IL) attached to a 26-gauge needle (Hamilton Co., Reno, NV) and 10 μl Hamilton syringe. Two microliters (10 μg/coordinate) of 6-OHDA were injected at two coordinates in the MFB: AP = −1.8 mm, ML = +2.0 mm, DV = −8.2 mm and AP= −2.8 mm, ML = +1.8 mm, DV = −8.2 mm (Paxinos and Watson, 2007). The needle was removed 5-min post-injection to prevent backflow. Given the established and standard nature of this model, both in the field and in our Laboratory, no sham-surgery groups were included.

2.4. Amphetamine-induced rotation test

To determine the severity of the 6-OHDA lesions, rats were treated with dextro-amphetamine (5 mg/kg in sterile 0.9% normal saline, *i.p.*; Sigma-Aldrich) and placed in a plexiglass cylinder (38 cm diameter × 38 cm height). Rotations (contralateral and ipsilateral to the lesion) were recorded for 1-min, every 5-min, over 100-min. The mean ± SEM net ipsilateral rotations were calculated and rats were assigned to balanced treatment groups. Only rats with a net ipsilateral rotation score ≥ 4 were included in each study ($n = 80$). In *Experiment 1*, one rat died and two were removed for unrelated health reasons. In *Experiment 2*, one rat was removed for its inability to perform the RotaRod test at pre-lesion baseline.

2.5. Drug and vehicle preparation

All systemic drugs were administered at a volume of 1 ml/kg *via intraperitoneal* (*i.p.*) injection. In *Experiment 1*, ketamine (20 mg/kg; VetOne), *R*-ketamine (10 mg/kg; Cayman Chemicals, Ann Arbor, MI), and L-DOPA (6 and 12 mg/kg; Sigma-Aldrich) combined with benserazide hydrochloride (14 mg/kg; Sigma-Aldrich) were formulated in the vehicle solution, 0.9% USP grade sterile saline (VetOne). Benserazide is a peripherally acting aromatic L-amino acid decarboxylase or DOPA decarboxylase inhibitor, which is unable to cross the blood–brain barrier, used to prevent conversion of L-DOPA to dopamine in the bloodstream. In *Experiment 2*, ketamine (20 mg/kg; VetOne) was formulated in the vehicle solution, 0.9% USP grade sterile saline (VetOne). In *Experiment 3*, ketamine (20 mg/kg; VetOne) and L-DOPA (6 mg/kg) combined with benserazide (14 mg/kg) were formulated in 0.9% USP grade sterile saline (VetOne). N-[2-[(2-oxoazepan-3-yl)carbamoyl]phenyl]-1-benzothiophene-2-carboxamide (ANA-12; 0.5 mg/kg; Tocris Bioscience, Minneapolis, MN) was dissolved in 5% DMSO, 55% polyethylene glycol 400 (PEG-400; Sigma-Aldrich), and 40% normal saline. ANA-12 is a tropomyosin receptor kinase B (TrkB)-receptor antagonist used to probe for involvement of the BDNF pathway (Cazorla et al., 2011).

2.6. L-DOPA-induced dyskinesia (LID) rating scale

The severity of LID was assessed by an investigator blinded to experimental conditions using the abnormal involuntary movement (AIM) rating scale, based on the work of Dekundy et al., 2007, and established in our laboratory (Flores et al., 2014; Bartlett et al., 2016; Flores et al., 2018). We initially had validated it in our laboratory with amantadine (40

mg/kg, *i.p.*). AIMs were each scored on a scale 0 (no AIMs) to 4 (severe and uninterruptible) for 1-min, every 20-min, over 180-min. Limb, axial, and orolingual (LAO) AIMs were scored and summed as a composite score.

2.7. Forelimb adjusting steps (FAS) test

The FAS test was used to measure akinesia. In *Experiments 1* and *3*, rats underwent testing pre- and post-lesion. Testing was performed following the first, fourth, and fifth (paired with L-DOPA) injections on each treatment day. Each test consisted of three trials performed at 40, 60, and 80 min post-injection of either ketamine or saline. In each trial, the hind limbs of the rats were raised, and one forepaw was restrained by the investigator. The rat was then moved laterally, with only the unrestrained forepaw supporting its body weight, across a smooth surface of 90 cm, at a rate of 9 cm/s. All behavioral testing sessions were video recorded and the mean ± SEM number of steps were counted by a blinded investigator, as published (Flores et al., 2018).

2.8. RotaRod test

The RotaRod test was used to investigate motor coordination in the unilateral 6-OHDA rat model as first shown by Monville et al., (2006). Using a modified version of the protocol published by Su et al., (2018), rats were trained on a 4-lane RotaRod (Rotamex 4/8, Columbus Instruments, Columbus, OH) for two consecutive days. Each training session consisted of a 5-min trial at a constant speed of 10 rotations per minute (rpm). Testing was then performed 7 days prior to the administration of 6-OHDA (Pre-Lx) and again at 28 and 35 days post-lesion (Post-Lx). Testing sessions were performed on an accelerating rod (4 to 40 rpm) and consisted of four, two-minute trials spaced 20 min apart. These were performed at 40, 60, 80, and 100 min post-injection of either ketamine or saline. The mean latency to fall from the first three time points was used for analysis.

2.9. Treatment groups and experimental design

In *Experiment 1*, PD rats were treated every seven-days with either vehicle, *R*-ketamine, or ketamine in accordance with our published (Bartlett et al., 2016; Ye et al., 2018) 10-h ketamine treatment-paradigm (Fig. 1A). To create the LID model on day 0, L-DOPA was paired with the 5th injection and then given each day throughout the remainder of the priming period (D0–13: 6 mg/kg; D14–49: 12 mg/kg). LAO-AIMs were scored every 3–4 days up to day 45. In *Experiment 2*, PD rats underwent a similar treatment protocol that omitted L-DOPA (Fig. 1B). In *Experiment 3*, rats underwent a similar treatment protocol (Fig. 1C); vehicle and ketamine injections were given five times, every two-hours on days 0 and 7 during the two-week priming with L-DOPA (6 mg/kg). ANA-12 was administered with the first injection and again five-hours later based upon evidence that peak TrkB receptor phosphorylation occurs at 4-h (Cazorla et al., 2011; Fischer et al., 2017).

2.10. Measurement of dopamine content

In *Experiment 1*, rats were euthanized on day 49 with carbon dioxide one hour after the fifth injection of ketamine paired with L-DOPA. The brains were extracted and coronal brain

slices, 1 mm thick, were collected, 2 mm steel biopsy punches were taken from the intact and lesioned striata and analyzed by HPLC-EC, as previously published (Flores et al., 2018).

2.11. Tissue preparation for western blot, multiplex immunoassays

In *Experiment 2* and the ANA-12-only control study, rats were euthanized on Day 14 with carbon dioxide. The remaining striatal tissue from *Experiment 1*, as well as the whole striatal tissue from *Experiment 2* and the ANA-12-only control study, was dissected from both hemispheres and flash frozen in liquid nitrogen. Tissue was homogenized in ice-cold phosphate buffered saline containing 1% Triton X-100, 0.1% sodium dodecyl sulfate, protease inhibitor cocktail at 1:100 (Sigma-Aldrich) and a phosphatase inhibitor cocktail tablet (Roche, Basel, Switzerland). Homogenate was centrifuged for 30-min at 14,000 g and aliquoted at −70 °C. Protein concentration was determined for each subsequent immunoassay using a BCA assay (ThermoFisher Scientific, Waltham, MA) and read on a FlexStation 3 (Molecular Devices, San Jose, CA).

2.12. Western blot analysis

All striatal tissue was run on Any-kD MiniProtean® TGX™ precast gels, transferred with a Trans-Blot TurboTransfer System (Bio-Rad Laboratories, Hercules, CA), Chameleon® Duo Pre-stained Protein Ladder was used for size reference, blots were scanned on an Odyssey CLx imaging system, (LI-COR, Lincoln, NE) and analyzed with Empiria Studio Software according to the manufacturers respective recommendations. Tissue homogenate samples from the striata of dyskinetic rats in *Experiment 1* were loaded with a two-fold dilution from 64 to 0.5 μg to determine a linear range for each protein, and 5–15 μg of protein was loaded on each gel with a positive and negative control. Primary antibodies: Phospho-p44/42 MAPK (ERK1/2) (Thr 202/Tyr 204) (L34F12) (1:2000), Pan-p44/42 MAPK (ERK1/2) (1:2000) (Cell Signaling Technology, Danvers, MA). Tyrosine Hydroxylase (1:2000) (Millipore, Billerica, MA). Beta-Actin (1:10,000) (Sigma-Aldrich). LICOR secondary antibodies: IRDye® 800 CW Donkey anti-Rabbit (1:10,000), IRDye® 680 CW Donkey anti-Mouse (1:10,000). Controls: p44/42 MAPK control cell extracts (Cell Signaling Technology).

2.13. mTOR pathway evaluation

Phospho-mTOR (Ser2448) and total mTOR levels were measured using a 2-plex magnetic bead panel kit (46–686MAG; Millipore). The immunoassay was performed according to the manufacturer's protocol with each sample, standard, and quality control measured in duplicate, using a MAGPIX system (Luminex, Austin, TX).

2.14. Tissue preparation for Golgi-Cox analysis and immunohistochemistry

In *Experiment 3*, rats were sacrificed on Day 14 of AIMs scoring, within 4-h of behavioral testing. They were deeply anesthetized with Euthanasia Solution (0.35 ml; VetOne) and transcardially perfused with 200 ml of heparinized (10 units per ml; Sagent, Schaumburg, IL) 0.9% normal saline, followed by 200 ml of cold paraformaldehyde (4% in 0.1 M phosphate buffer (PB); MP Biomedicals, Santa Ana, CA). Brains were extracted and hemisected at the hypothalamus. The rostral half, containing the striatum, was post-fixed

in paraformaldehyde for 1-h, then shipped overnight in 0.1 M PB to Dr. Steece-Collier. To validate severity of the 6-OHDA lesion, 40 μm sections yielding the SN were obtained using a cryostat (CM1850, Leica, Wetzlar, Germany), and IHC was performed as described in prior work (Flores et al., 2018). Sections were incubated with rabbit anti-TH primary antibody (1:1000; AB152; Millipore) at 4 °C overnight and a biotinylated goat anti-rabbit IgG secondary antibody (1:4000; AP187B; Millipore) for 2-h at RT, followed by ABC reagent (Vectastain Elite ABC Kit; PK-6100; Vector Laboratories, Burlingame, CA). TH-ir neurons were visualized using a DAB Kit (SK-4100; Vector Laboratories). Densitometry analysis of the total area of detected objects (total pixels2) in a 480 × 480 pixel region of the mediolateral SN (3 sections/rat) was conducted by a blinded investigator with ImageJ software (*vs.*2.0.0-rc-69/1.52p, http://rsbweb.nih.gov/ij/) according to an established protocol (Kneynsberg et al., 2016).

2.15. Golgi-Cox impregnation and analysis

All procedures and methods performed for Golgi-Cox impregnation and dendritic spine analysis were performed based on previously established criteria developed in the laboratory of Dr. Steece-Collier (Zhang et al., 2013; Levine et al., 2013). Upon arrival at Michigan State University, the rostral half of the brain was impregnated using a modified Golgi-Cox protocol, sectioned at 100 μm on a vibrating microtome (VT1000S; Leica Microsystems), and mounted on gel-coated slides. Golgi-impregnated neurons from the dorsolateral part of the precommissural, commissural, and dorsal striatum were initially identified at low-power magnification. For analysis, only neurons with at least 4 primary dendrites radiating from the soma in a 360° arc with no overlap with adjacent cells were selected. A single dendrite from a neuron in each region of the striatum (3 dendrites/hemisphere/rat) was traced and spine density, length, and phenotype were quantified by a blinded investigator using Neurolucida® (MBF Bioscience, Williston, VT).

2.16. Bladder pathology

Urinary bladders were fixed in 10% buffered formalin, processed, paraffin-embedded, and 5 μm sections were stained with hematoxylin and eosin. All slides were evaluated by a board-certified veterinary pathologist (DB) blinded to the experimental design and sample group assignment. Lesion interpretation was performed in accord with a previously published lesion scoring system (Gu et al., 2014).

2.17. Statistical analyses

Statistical analyses were performed using GraphPad Prism 8.0 software (GraphPad Software, La Jolla, CA). The null hypothesis was rejected when $p < .05$. All values are represented as mean ± SEM. Dopamine content and TH-ir densitometry were analyzed with two-way ANOVAs and Bonferroni *post hoc* tests. LAO-AIMs were analyzed with non-parametric Kruskal-Wallis tests with Dunn's multiple comparisons *post hoc* tests. FAS and RotaRod tests were analyzed with ANOVAs with Tukey-Kramer corrected *post hoc* tests. Western blot and mTOR analyses were performed with two-tailed *t*-tests on data before normalization to vehicle control. Spine data was analyzed with one-way ANOVA with Sidak's multiple comparisons test. Correlations were performed with Pearson's correlations. A summary with all statistical details is presented in the Appendix A.

3. Results

3.1. Post hoc analyses, verification of the hemi-parkinsonian 6-OHDA lesions

In prior work we have shown that injection of 6-OHDA into the medial forebrain bundle (MFB) leads to a > 90% reduction in striatal DA content, with no adverse effects on serotonin levels or metabolites (Flores et al., 2014; Bartlett et al., 2016; Flores et al., 2018). The rats included in *Experiment 1* (Fig. 1A) showed a mean (±SEM) number of amphetamine-induced ipsilateral rotations per minute of 8.49 ± 0.49, and the rats included in *Experiment 2* (Fig. 1B) performed at 8.86 ± 1.19 rotations per minute. The rats included in *Experiment 3* (Fig. 1C) performed at 6.36 ± 0.21 rotations per minute, and the rats included in the ANA-12-control study showed 6.69 ± 0.41 rotations per min. These values indicate strong (> 90% DA loss) hemi-parkinsonian lesions. Post-mortem analyses using high pressure liquid chromatography with electrochemical detection (HPLC-EC) confirmed > 95% loss of striatal DA on the lesioned compared to the intact side for *Experiment 1* ($F[1,48] = 393$, $p < .001$, two-way ANOVA, Bonferroni *post hoc* tests; Fig. 1D). In *Experiment 2*, semi-quantitative western analysis of striatal tissue using tyrosine hydroxylase (TH) as a marker for DA terminals was used to evaluate the severity ($t = 13.60$, df = 16, $p < .001$; two-tailed *t*-test) of the lesion (Fig. 1E). In *Experiment 3,* brains were processed for TH immunoreactivity (TH-ir) as a marker of SN DA neurons following immunohistochemical (IHC) staining, and densitometry quantification revealed > 95% reduction in the lesioned hemispheres in *Experiment 2* ($F[1,54] = 150$, $p < .001$, two-way ANOVA, Bonferroni *post hoc* tests; Fig. 1F,G). Semi-quantitative western analysis of striatal tissue using TH was used to evaluate the severity ($t = 17.21$, df = 18, $p < .001$; two tailed *t*-test) of the lesion in the ANA-12-only control study (Fig. 1H). Given a recent publication that ketamine abuse can lead to pathological changes in urinary bladder tissue (Gu et al., 2014), we also evaluated urinary bladders for pathology after our repeated ketamine-treatments in *Experiment 3*. We found no significant pathological changes using hematoxylin and eosin staining in ketamine-treated rats as compared to rats administered vehicle control (Table 2).

3.2. Ketamine attenuates L-DOPA-induced dyskinesia

In *Experiment 1* we investigated the ability of ketamine treatment to attenuate the development of LID in a rodent model of PD. Here we used our previously published treatment paradigm (Bartlett et al., 2016; Ye et al., 2018) to investigate whether weekly administration of a 10-h ketamine exposure could attenuate the development of dyskinesia during a seven-week L-DOPA priming period (Fig. 2A). L-DOPA-induced limb, axial, and orolingual abnormal involuntary movements (LAO-AIMs) were compared between treatment groups every 3–4 days during a four-week priming period with escalating doses of L-DOPA (6 and 12 mg/kg) (Fig. 2A). A Kruskal-Wallis test with Dunn's multiple comparisons *post hoc* tests was used to compare the effect of treatment on LAO-AIMs (mean ± SEM). In the first week of priming with 6 mg/kg of L-DOPA, the total LAO-AIMs scores of LID-rats treated with ketamine (D0: 2.00 ± 1.15; D3: 17.00 ± 6.88) were markedly attenuated on days 0 and 3 compared to vehicle (D0: 12.00 ± 4.18; D3: 34.44 ± 4.02) (Fig. 2A) by 83% and 51%, respectively. The anti-dyskinetic effect was maintained into the

second week, where ketamine (15.00 ± 6.75) significantly reduced total LAO-AIMs by 63% on day 7 compared to vehicle (41.00 ± 5.78; $H = 6.59$, $p < .05$, $n = 9$).

We next tested the ketamine enantiomer, *R*-ketamine. On day 11, ketamine (the racemic mixture) maintained a 64% reduction in LAO-AIMs (11.06 ± 3.73) compared to vehicle (30.50 ± 5.46; $H = 9.12$, $p = .07$, $n = 9$); however the effect of *R*-ketamine was not significantly different than that seen in vehicle (34.56 ± 5.47; $n = 9$) treated group. These results were mirrored in the LID-expressing rats when challenged with a higher dose of L-DOPA (12 mg/kg) for the last ten testing sessions of *Experiment 1*. LAO-AIMs were reduced between 40 and 55% in rats treated with racemic ketamine on all days (D14: 37.78 ± 10.91; D17: 31.61 ± 9.27; D21: 29.33 ± 8.93; D25: 27.61 ± 7.33; D28: 25.61 ± 6.81; D31:25.22 ± 6.12; D35: 23.22 ± 7.73; D39: 25.50 ± 8.33; D42: 24.06 ± 7.42; D45: 25.44 ± 6.59) compared to vehicle (D14: 62.72 ± 6.47; D17: 59.22 ± 4.47; D21: 54.72 ± 5.43; D25: 52.89 ± 5.58; D28: 52.28 ± 5.22; D31: 47.67 ± 4.65; D35: 48.83 ± 5.63; D39: 54.94 ± 3.94; D42: 53.78 ± 3.72; D45: 51.83 ± 4.34), with the effect of ketamine reaching significant difference from vehicle on day 28 ($H = 9.40$, $p < .05$, $n = 9$) and remaining so throughout the study (D31:$H = 10.29$, $p < .05$; D39:$H = 6.18$, $p < .05$; D42:$H = 8.45$, $p < .05$; D45:$H = 9.17$, $p < .05$, $n = 9$ each). As with the lower dose of L-DOPA, *R*-ketamine treatment did not produce a reduction of LAO-AIMs compared to vehicle. Racemic ketamine significantly reduced LAO-AIMs 47–58% compared to *R*-ketamine on days 25 (51.78 ± 7.18; $H = 7.94$, $p < .05$), 28 (51.50 ± 7.07; $H = 9.40$, $p < .05$), 31 (50.50 ± 6.89; $H = 10.29$, $p < .05$), 35 (55.33 ± 7.73; $H = 8.46$, $p < .05$), 45 (52.78 ± 7.47; $H = 9.17$, $p < .05$, $n = 9$ each).

The time course plots of *Experiment 1* show that the effects of ketamine on LAO-AIMs occur throughout the first 2-h of behavioral testing, while L-DOPA is active (Fig. 2, B and C). Kruskal-Wallis tests with Dunn's multiple comparisons *post hoc* tests were used to compare the effect of treatment on LAO-AIMs (mean ± SEM) at each time point. Days 11 and 25 readily revealed the long-term effects of ketamine and thus were used to examine potential difference in the daily time course of LID expression between groups. On day 11, total LAO-AIMs were significantly reduced ($n = 9$ each) by ketamine (20′: 0.56 ± 0.19; 40′: 3.06 ± 1.03; 60′: 2.56 ± 1.12), compared to vehicle (20′: 4.67 ± 1.12; 40′: 8.17 ± 1.24; 60′: 7.22 ± 1.26), at 20 ($H = 8.35$, $p < .05$, 88%-reduction), 40 ($H = 9.32$, $p < .01$, 63%), and 60 ($H = 9.32$, $p < .05$, 65%) minutes post-L-DOPA injection. In the following hour, ketamine also reduced LAO-AIMs at the 80 and 100-min time points compared to vehicle. Again, there was no effect of *R*-ketamine at any time point. However, there was a reduction of LAO-AIMs by ketamine compared to *R*-ketamine at minute 20, which reached significance at the next three time points ($n = 9$ each), 40 (7.83 ± 1.07; $H = 9.32$, $p < .01$), 60 (8.44 ± 1.22; $H = 9.32$, $p < .01$) and 80 (7.78 ± 1.41; $H = 6.34$, $p < .05$) minutes. Similar to day 11, ketamine also reduced LAO-AIMs for the first 2 h of the behavioral testing on day 25. Compared to vehicle there was a reduction by ketamine evident in LAO-AIMs at 20, 40, 60, 80, and 100-min when challenged with the higher dose of L-DOPA. The effect of ketamine (1.61 ± 0.45) reached significance compared to vehicle (6.33 ± 1.15) at 120 ($H = 8.61$, $p < .05$, $n = 9$, 75%-reduction) minutes. Individual limb, axial, and orolingual (Fig. 3A–C) scores showed similar reductions of specific sub-categories of L-DOPA-induced AIMs suggesting that there was not one single type of AIMs driving the effects of ketamine.

3.3. Ketamine does not interfere with L-DOPA activity and has an acute anti-parkinsonian activity

One possible explanation of the anti-dyskinetic benefit of ketamine, is that it simply suppresses striatal DA release, rather than improving the therapeutic range of L-DOPA. To test this possibility, we used the forelimb adjusting steps (FAS) test as a measure of akinesia after the first, fourth, and fifth injections of ketamine during the 5-injection sequence that comprised the 10-h treatment period. This test revealed that L-DOPA in the presence of ketamine does not appear to interfere with the anti-PD activity of L-DOPA, and actually has motoric benefit independent of L-DOPA. Specifically, in parkinsonian rats there is a reduction in the number of adjusting steps (mean ± SEM; repeated measures one-way ANOVA, Tukey multiple comparisons *post hoc* tests) made by the forelimb contralateral to the lesion when the rat is moved laterally (Fig. 4A). We found that this impairment was reversed by L-DOPA in both ketamine-treated rats $F[1.83,14.63] = 34.74$, $p < .001$), and vehicle-treated rats ($F[1.77,14.18] = 51.86$; $p < .05$, $n = 9$) when compared to the number of steps taken post-lesion in the absence of drug treatment. Additionally, acute ketamine injections were noted to improve stepping independent of L-DOPA (Fig. 4A). The 1st (0.41 ± 0.09; $F[1.59,12.79] = 5.28$; $p < .05$, $n = 9$) and 4th ketamine (0.37 ± 0.06; $F[1.59,12.79] = 5.28$; $p < .05$, $n = 9$) injections in the 10-h treatment protocol improved akinesia by 66% and 62%, respectively, as compared to post-lesion steps in the absence of drug treatment (0.14 ± 0.02). Unpaired two-tailed sample *t*-tests revealed that the 1st ($t = 2.57$; $p < .05$, $n = 9$) and 4th ($t = 2.22$; $p < .05$, $n = 9$) injections of ketamine significantly increased the number of steps compared to the respective vehicle controls. To further evaluate if the effects of ketamine are truly anti-parkinsonian, and not only anti-akinetic, unilateral 6-OHDA-lesioned PD rats treated with ketamine were challenged with the RotaRod test (Fig. 4B), a more complex test and better assessment of motor skills. Post-lesion the latency to fall was reduced by 50% compared to pre-lesion baseline in the PD animals ($F[1.98,15.81] = 78.35$; $p < .05$, $n = 9$). Ketamine treatment completely restored the ability of PD rats to perform on the RotaRod already at the 1st injection (Fig. 4B).

3.4. Ketamine-treatment activates the striatal ERK1/2 and mTOR pathways

Post hoc analysis revealed that neither ketamine, nor *R*-ketamine, had a significant effect on striatal DA content in either the intact or lesioned striatum (Fig. 1C). This suggests that the anti-dyskinetic effect is down-stream of the DA receptor. In order to probe the effects of ketamine on these downstream signaling mechanisms, we examined two intracellular messenger pathways for these initial proof-of-principle studies. It has been shown that mTOR signaling is involved in the therapeutic effect of ketamine in preclinical depression models (Welberg, 2010; Akinfiresoye and Tizabi, 2013), and we now provide data in our model system using a multiplex immunoassay demonstrating increased mTOR phosphorylation by ketamine (unpaired two-tailed *t*-tests, $n = 9$) in both the intact ($t = 5.08$; $p < .001$) and lesioned ($t = 2.88$; $p < .05$) striatum 1-h after ketamine (Fig. 5A,B). Western blot analysis showed a similar effect of ketamine on the ERK1/2 pathway, increasing phosphorylation of the Thr202/Tyr204 site (unpaired two-tailed *t*-tests, $n = 9$) in both the intact ($t = 2.45$; $p < .05$) and lesioned ($t = 2.26$; $p < .05$) striata (Fig. 5C-E).

3.5. The anti-dyskinetic effect of ketamine is BDNF dependent

In *Experiment 3* we confirmed the same anti-dyskinetic effect with our 10-h ketamine-treatment paradigm (Fig. 1C) as reported for *Experiment 1*. However, here we examined the impact of N-[2-[(2-oxoazepan-3-yl)carbamoyl]phenyl]-1-benzothiophene-2-carboxamide (ANA-12), an antagonist of the BDNF receptor, TrkB (Cazorla et al., 2011; Fischer et al., 2017), on the anti-dyskinetic efficacy of ketamine. L-DOPA-induced LAO AIMs (mean ± SEM) were compared between rats receiving ketamine or ketamine plus ANA-12 (Fig. 6A) every 3–4 days during a two-week priming period with a single dose of L-DOPA (6 mg/kg). As we have noted previously, total LAO-AIMs scores in rats treated with ketamine (D0: 0.60 ± 0.36, 94% reduction; D7: 10.65 ± 3.36, 65% reduction; D11: 13.85 ± 3.81, 55% reduction; D14: 15.85 ± 3.85, 57% reduction) were significantly reduced compared to vehicle controls (D0: 9.55 ± 3.8; D7: 30.50 ± 3.65; D11: 30.75 ± 1.69; D14: 37.10 ± 3.45) on days 0 (H = 6.23, p < .05, n = 10, Kruskal-Wallis test with Dunn's multiple comparisons *post hoc* tests), 7 (H = 8.24, p < .05, n = 10), 11 (H = 9.37, p < .05, n = 10), and 14 (H = 9.44, p < .01, n = 10). These data also demonstrate the long-term, BDNF dependent effects of ketamine, as LAO-AIMs were considerably reduced after the first 10-h treatment compared to rats treated with both ketamine and ANA-12. By comparison to rats receiving both ketamine and ANA-12, ketamine alone reduced LAO-AIMs on days 0 (0.60 ± 0.36, 80% reduction), 4 (14.70 ± 4.09, 39% reduction), 7 (10.65 ± 3.36, 46% reduction), 11 (13.85 ± 3.81, H = 9.4, p = .06, 50% reduction), and this reduction reached significance by day 14 (15.85 ± 3.85; H = 9.4, p < .01, 52% reduction) as compared to the ANA-12 treated rats. The daily time course of LID behavior for *Experiment 3* shows that the anti-dyskinetic effect of ketamine remains during the full duration of L-DOPA activation (Fig. 6B). LAO-AIMs showed a non-significant reduction in the first 40 min before reaching significance with ketamine treatment at the 60 (4.30 ± 1.02; H = 9.32, p < .01, 52% reduction), 80 (2.40 ± 0.80; H = 13.30, p < .01, 73% reduction), and 100 (0.95 ± 0.59; H = 7.39, p < .05, 76% reduction) minute time points compared to vehicle (60′: 9.05 ± 0.73; 80′: 8.90 ± 0.89; 100′: 4.0 ± 1.06) on day 14. Ketamine (2.40 ± 0.80) also significantly reduced LAO-AIMs compared to the ANA-12 (7.35 ± 1.08) treated group at 80 min (H = 13.30, p < .05, 67% reduction). The ANA-12-only control experiment (Fig. 6C) clearly shows that ANA-12-only treatment had no individual effect on LID development, as the mean ± SEM LAO-AIMs (D0: 17 ± 3.9; D4: 31 ± 6.2; D7: 37 ± 3; D11: 29 ± 3.5) in this group do not differ from the vehicle groups of either *Experiment 1* or *3*. Together, these data demonstrate that the anti-dyskinetic effect of ketamine is critically dependent on the activation of BDNF signaling. Ketamine reduced individual limb, axial, and orolingual (Figs. 7A-C) AIMs compared to both vehicle and ketamine + ANA-12 treated rats, again indicating that the effect was not driven by a specific subtype of AIMs.

3.6. Ketamine reduced dendritic mushroom spines in the dyskinetic striatum

We have previously shown that the anti-dyskinetic effect of ketamine remained over several weeks post-ketamine treatment in a model of established LID (Bartlett et al., 2016). In the current study we extended our previous studies by examining whether ketamine could attenuate the development/induction of LID and whether the effect was long-term. The anti-dyskinetic effect of ketamine is evident for up to a week after the final ketamine treatment, suggesting that these long-term effects may be related to structural neuroplasticity. Ketamine

treatment leads to dendritic spine changes in preclinical models of depression. Further within the dyskinetic striatum in the unilateral rat model there is an increased density of mushroom spines (Zhang et al., 2013). Therefore, we employed Golgi impregnation methods to examine the impact of L-DOPA in the presence or absence of ketamine on striatal dendrites and spines. Analysis of dendrite length showed no significant difference between treatment groups (Fig. 8A). Our data (Fig. 8B-E) replicated, and extended, our previously published findings that L-DOPA caused an increase in the number of mushroom spines in the dyskinetic striatum (Zhang et al., 2013; Nishijima et al., 2014). Specifically, in the lesioned striatum of LID-expressing rats treated with ketamine the mushroom spine density (0.75 ± 0.11) was significantly reduced ($F[2,27] = 22.82$, $p < .001$, $n = 10$) by 52% compared to vehicle treatment (1.55 ± 0.09), resulting in similar numbers to that of the intact striatum (0.79 ± 0.04) in the vehicle controls. In agreement with our hypothesis that the anti-dyskinetic effect of ketamine is dependent on BNDF signaling, blocking TrkB reversed the effects of ketamine in decreasing the number of mushroom spine in the lesioned striatum resulting in ANA-12 (1.52 ± 0.08) treated rats showing a significant ($F[2,27] = 22.82$, $p < .001$, $n = 10$) increase in mushroom spine density comparable to L-DOPA treatment alone. These data support the idea that BDNF signaling as a critical mechanism in the long-term anti-dyskinetic effects of ketamine both on a structural as well as functional level.

In addition to changes in spine plasticity in the lesioned striatum there were unexpected treatment effects on mushroom spines in the contralateral intact striatum. Similar to the lesion side, ketamine (0.39 ± 0.03) significantly reduced (one-way ANOVA, $F[2,27] = 23.24$, $p < .001$, $n = 10$) mushroom spine density compared to vehicle (0.79 ± 0.04) and this effect was reversed in the presence of ANA-12 (0.67 ± 0.05). No significant differences were found between the vehicle and ANA-12 groups for either the intact or lesioned striata. However, significant within-group effects for each drug treatment were found (Fig. 8B). Specifically, mushroom spine density in the lesioned striatum was significantly increased compared to the intact striatum in the vehicle ($t = 7.77$; $p < .001$, $n = 10$), ketamine ($t = 3.08$; $p < .01$, $n = 10$), and ANA-12 ($t = 9.03$; $p < .001$, $n = 10$) treated groups (unpaired two-tailed sample *t*-tests).

Enlarged mushroom spines receiving multiple excitatory contacts have been shown to be increased in the striatum of dyskinetic rats (Zhang et al., 2013). Here we evaluated the correlation between total LAO-AIMs and the density of mushroom spines per 10 μm in the striata of both the intact and lesioned striata (Fig. 9A-F). In the lesioned striatum, there was a significant positive correlation between mushroom spine density and LAO-AIMs in the vehicle ($r = 0.72$, $p = .02$), ketamine ($r = 0.86$, $p = .001$), and ANA-12 plus ketamine ($r = 0.71$, $p = .02$) conditions. Neither vehicle nor ketamine-alone conditions on the intact side showed any correlation with LID, yet there was a positive significant correlation on the intact side of the ANA-12 plus ketamine ($r = 0.69$, $p = .03$) group. While there was a strong correlation of mushroom spines and LID, the thin spines did not correlate with the severity of LID (Table 3).

4. Discussion

Pharmacological studies have identified a role for glutamatergic signaling, and specifically for *N*-methyl-D-aspartate receptor (NMDAR)-mediated signaling in the development of LID (Sgambato-Faure and Cenci, 2012; Huot et al., 2013), and research into novel NMDAR antagonists for LID treatment have led to FDA approval of an extended-release formulation of amantadine, a drug with a weak NMDAR antagonism activity. However, amantadine is effective only for a subset of patients, can cause psychiatric disturbances, and there is no evidence that it provides long-term neuroplastic benefit (Rascol et al., 2015). Ketamine, a well-established NMDAR antagonist with greater binding affinity than amantadine (Bresink et al., 1995), has been utilized clinically as an anesthetic since 1970, and has recently been repurposed at sub-anesthetic doses for the treatment of chronic pain (Niesters et al., 2014) and depression (Andrade, 2017), with *S*-ketamine now being an FDA approved drug for use in treatment-resistant depression (Kaufman, 2019).

In the current set of studies, we tested whether sub-anesthetic ketamine or the enantiomer, *R*-ketamine, could also effectively suppress the development of AIMs when given from the outset of L-DOPA priming. The racemic mixture of ketamine significantly attenuated the development of AIMs when parkinsonian rats were treated with L-DOPA. In contrast, *R*-ketamine, which had been shown to be a potent antidepressant with less psychomimetic liability (Yang et al., 2015) had no anti-dyskinetic effect. This suggests that, in our model, the *S*-ketamine enantiomer is necessary for anti-dyskinetic efficacy. Indeed, there is some precedence to explain why *R*-ketamine was not anti-dyskinetic. *S*-ketamine has an approximately 2- to 3-fold higher affinity for NMDARs, and is a more potent analgesic (Suppa et al., 2012) and anesthetic (White et al., 1985) than racemic or *R*-ketamine. Moreover, *S*-ketamine has been shown to provide a rapid antidepressant effect in patients and was designated a '*Breakthrough Therapy*' (Kaufman, 2019).

We also importantly demonstrate that ketamine does not inhibit the pro-kinetic effects of L-DOPA, as the combination of L-DOPA + ketamine restored forelimb step adjusting behavior of the akinetic forelimb back to baseline/normal levels. Prior data from our group has already established that the same ketamine-treatment paradigm does reduce L-DOPA-induced LAO-AIMs in rats with prior established LID but does not acutely reduce L-DOPA-induced locomotor AIMs (Bartlett et al., 2016), while inducing locomotor activity in naïve healthy animals lasting 50 min for each low-dose ketamine injection (Ye et al., 2018). This locomotor activity was eliminated and ketamine-induced gamma oscillations in motor cortex were reduced by dopamine 1 receptor (D1R) antagonism. Repeated low-dose ketamine exposure was also shown by others to induce enduring resilient-like responses in adult rats (Parise et al., 2013). Interestingly, our data further demonstrate that ketamine can independently provide anti-parkinsonian benefit, as demonstrated by a significant increase in the number of steps by the impaired limb in the presence of ketamine in the absence of L-DOPA. Ketamine also reduced PD lesion-induced deficits on the RotaRod, a more complex test of PD motor deficits. These acute anti-parkinsonian effects support our prior clinical PD case study (Sherman et al., 2016), where sub-anesthetic ketamine infusion was not only anti-dyskinetic but also acutely improved motor symptoms in an individual with PD, and also in a second patient case study showing that a bolus dose (20 mg) of ketamine

given intravenously, in a preoperative setting, abolished tremor and dysarthria (Wright et al., 2009). A similar reduction of both tremor and dyskinesia was also seen in two patients given a combination of ketamine and the μ-opioid receptor agonist, remifentanil (Salazar and Motamed, 2012).

Ketamine acts as an antidepressant in humans (Andrade, 2017), and in animal models of depression rapidly reverses spine atrophy in the medial prefrontal cortex (PFC) and hippocampus (Qiao et al., 2016; Widman and McMahon, 2018; Treccani et al., 2019). In this respect, it is of importance that cellular dendritic spine changes in the striatum have been identified in the 6-OHDA model of PD, specifically a retraction of cortico-striatal inputs and spine atrophy on striatal medium spiny neurons (MSNs). Zhang and colleagues have shown that chronic administration of L-DOPA, resulting in LID, leads to the appearance of synaptic mis-wiring that include the reestablishment of the cortico-striatal inputs and spine density, however with pathological changes in distribution of these afferent inputs and increased numbers of mushroom spines on MSNs (Zhang et al., 2013).

In the current study we confirmed that dyskinogenic L-DOPA restored spine density to that of the intact, control hemisphere in vehicle treated rats and that this coincided with an expected increase in mushroom spines in the lesioned striatum. While a relationship between L-DOPA treatment and enlarged, mushroom-like spines has been previously suggested (Shen et al., 2008; Belujon et al., 2010; Zhang et al., 2013; Nishijima et al., 2014), to the best of our knowledge this is the first report of a direct and statistically significant correlation between mushroom spine density in the lesioned striatum and LID severity. These data implicate mushroom spine pathology as a possible structural marker for determining the efficacy of novel treatments for dyskinesia. The biological relevance of this finding is further supported by our data showing that sub-anesthetic ketamine, which attenuated AIMs, also attenuated the induction of mushroom spines, resulting in the same mushroom spine density in the parkinsonian striatum of rats receiving ketamine + L-DOPA as seen in the intact side of the control rats. These data demonstrate that ketamine has a robust effect on LID behavior as well as aberrant L-DOPA-induced neuroplasticity, specifically dendritic spine morphology which is known to be a critical attribute of striatal circuitry. Since we utilized Golgi staining methods we were not able to discern if there are specific differential effects of ketamine on direct *vs.* indirect pathway MSNs, yet there is clearly a significant functional impact of global increases in striatal mushroom spines. The loss of spines and their cortico-striatal connections occurs specifically in the indirect pathway MSNs in the parkinsonian state (Yagishita et al., 2014), and long-term potentiation (LTP) is changed and unstable at indirect but not direct pathway MSNs in the dyskinetic striatum (Suarez et al., 2016). Therefore, one could speculate that changes in indirect pathway MSNs might be not only an important feature of the dyskinetic striatum, but also important for the anti-dyskinetic action by ketamine. It cannot be ruled out that some striatal neurons in the parkinsonian brain have still a residual ability to correctly respond to L-DOPA with a bidirectional plasticity. Since individuals with PD come with variable striatal damage and amount of residual mushroom spines, and given the effect of ketamine to slightly decrease mushroom spines on the intact side as well, a note of caution is warranted as we cannot rule out that this could lead to side effects that may limit its use in some

individuals with PD, possibly requiring implementation of co-treatments to protect valuable residual functions.

In an effort to unmask the underlying mechanisms responsible for the neuroplastic changes associated with ketamine, we used the molecular road map provided by the depression literature. An abundance of evidence has demonstrated that BDNF plays an important role in neuroplasticity and depression (Bramham and Messaoudi, 2005; Castrén and Antila, 2017). Serum BDNF levels have been shown to be significantly lower in patients with major depressive disorder (Gonul et al., 2005). In rodent models, a conditional knockout of the BDNF gene in the forebrain of mice results in depression in both sexes (Monteggia et al., 2007). It has also been shown that an intracerebral injection of BDNF into the hippocampus acts as an antidepressant (Shirayama et al., 2002). BDNF is a well-known regulator of spine density *via* ERK1/2 activation (Alonso et al., 2004). The rapid antidepressant effects of ketamine have been shown to be dependent on BDNF synthesis in a mouse model of depression (Autry et al., 2011). In the current study, we tested the hypothesis that BDNF is necessary for the anti-dyskinetic effects of ketamine by co-administering the TrkB receptor antagonist ANA-12 with ketamine during the 10-h treatment. We chose ANA-12 as it was shown after systemic (*i.p.*) administration to cross the blood–brain barrier, to preferentially diffuse into the striatum and reduce TrkB signaling without affecting the survival of neurons in naïve rodents (Cazorla et al., 2011). TrkB signaling has been shown to be important in a variety of physiological processes such as learning and reward, while abnormal BDNF-mediated activation of TrkB has been reported in some psychiatric disorders. Trophic effects of TrkB activation are mostly associated with a positive outcome, yet can also be associated with neuropathic pain, drug abuse and epilepsy (as reviewed in Boulle et al., 2012). In our control study we show that systemic administration of ANA-12-only using the same once weekly 10-h treatment paradigm had no effect on LID development, arguing against effects by blocking BDNF-signaling globally in this rat model of the LID development. But, as predicted, blocking BDNF binding prevented the anti-dyskinetic effect of ketamine, resulting in LID development similar to that seen in parkinsonian rats treated with L-DOPA in the absence of ketamine. Further blocking BDNF binding to TrkB receptors with ANA-12 also prevented the increased mushroom spine density in the parkinsonian dyskinetic striatum. As discussed above, ketamine reduced these spines by approximately 50% compared to controls, while the rats treated with L-DOPA + ketamine + ANA-12 showed a significant increase in mushroom spines to the same level as seen with L-DOPA alone. Since ketamine and ANA-12 were given systemically we cannot rule out that additional morphological changes outside the striatum could contribute to the anti-dyskinetic effects seen, but our assertion of BDNF-signaling involvement in the ketamine effects in the LID model is complemented by the fact that BDNF-signaling has been identified as an important mechanism of the antidepressant activity by ketamine in depression (Hashimoto, 2020).

It is proposed that the antidepressive activity of ketamine, which depends on activating BDNF release, leads to changes in both the ERK and PI3K-Akt pathways that converge to phosphorylate mTOR (Harraz et al., 2016), a main regulator of neuroplasticity (Lipton and Sahin, 2014). This has been demonstrated in rat models of depression, in which phosphorylated ERK1/2 is upregulated in response to ketamine in the prefrontal cortex (Li

et al., 2010). This study, as well as others, have also identified downstream activation of mTOR in response to ketamine (Li et al., 2010; Harraz et al., 2016) and that this may lead to changes in spine density. We confirmed in the current studies the activation of both the ERK1/2 pathway and the mTOR pathway in the striatum in response to the 10-h ketamine treatment paradigm. Increase in the ERK1/2 pathway has been shown to correlate with LID (Ding et al., 2011) and inhibition of mTOR has been shown to reduce LID (Decressac and Björklund, 2013), which on the surface seems contradictory. But both the maladaptive sprouting underlying the dyskinetic state and the long-term reversal, *i.e.* the replacement of maladaptive striatal mushroom spines with monosynaptic thin spines after ketamine-treatment, are neuroplastic changes in dendritic striatal spines, therefore it is perhaps not surprising that the canonical mTOR and ERK1/2 pathways known to regulate neuroplasticity (Reichardt, 2006; Lipton and Sahin, 2014) can be involved in both opposing events. After all synaptic input is a highly dynamic process linked to morphological spine changes (Bosch and Hayashi, 2012). Alternatively, it is possible that differences of p-ERK1/2 or p-mTOR in a particular subset of striatal neurons or differential MAP kinase pathway regulation in different parts of the striatum in response to ketamine could also underlie the effects. Based on the *disinhibition hypothesis* (Miller et al., 2016; Zanos and Gould, 2018), ketamine is thought to selectively antagonize NMDARs located on cortical interneurons. We propose that there might be a similar cascade in the anti-dyskinetic action of ketamine, but involving different neural networks, as outlined in the scheme in Fig. 10. We focus on the cortical parvalbumin (PV)-positive interneurons as initiator of the action, though we cannot rule out an involvement of striatal PV-positive interneurons in the action of ketamine. We base this interpretation of the BDNF-dependent response on the fact that while cortical principal neurons can produce BDNF, it is well established that striatal BDNF derives from cortical and nigral projections, as striatal MSNs do not produce BDNF themselves (Altar et al., 1997). Since the nigral projections in the 6-OHDA-model we use are reduced be > 95% the source of the vast majority of the BDNF has to be from cortical projections. In contrast to our findings, it has been shown that exogenous overexpression of BDNF in the striatum using a viral vector and driven by a strong constitutive viral promoter can increases the susceptibility to LID (Tronci et al., 2017). The maladaptive plasticity due to such a strong global non-physiological overexpression of BDNF in the whole striatum differs from what we see in our case, where there is a physiological release of BDNF due to activation of cortico-striatal projections, leading to focal changes that reverse maladaptive plasticity, which could explain these differences. In addition, the known upregulation of cortical BDNF and striatal TrkB in hemi-parkinsonian animals after L-DOPA-treatment (Guillin et al., 2001) could actually make the cortico-striatal system even more responsive to the long-term anti-dyskinetic action of ketamine. Alternatively, tissue specificity of the BDNF-dependent effects of ketamine action within the striatum cannot be ruled out.

A further limitation of the current studies is that, while these data clearly suggest a role for BDNF signaling in the action of ketamine, mirroring that shown to underlie its antidepressive mechanism (Zanos and Gould, 2018), other mechanism are likely also involved. Indeed, ketamine is a multifunctional ligand interacting with multiple receptor targets, including agonism of the μ/δ-opioid receptors. Opioid systems are known to be altered in LID (Fox et al., 2006; Samadi et al., 2006) and ketamine binds to opioid receptors

with an affinity similar to NMDAR (Finck and Ngai, 1982). The antinociceptive activity of ketamine can be blocked by antagonizing opioid receptors (Pacheco et al., 2014). In a recent study, the antidepressive activity of ketamine was also reduced by an opioid receptor antagonist (Williams et al., 2018). Therefore, we cannot rule out that while NMDAR antagonism with ketamine produces long-term anti-dyskinetic effects without inducing pro-PD activity, its co-activation of the opioid system could also be important in the action of ketamine. In support of this, the highly-specific non-competitive NMDAR antagonist MK-801 (Paquette et al., 2010; Flores et al., 2014), while being acutely anti-dyskinetic, also induces the undesired consequence of pro-parkinsonian effects. Compellingly, recent data show that the combination of MK-801 with MMP-2200, a mixed μ/δ-opioid receptor agonist, blocks the pro-parkinsonian features of MK-801 without interfering with its anti-dyskinetic properties (Flores et al., 2018).

In conclusion, data presented here support further investigation into repurposing sub-anesthetic ketamine treatment for individuals with PD who are afflicted with LID. A small series of PD patient case reports have already demonstrated initial safety and feasibility in this patient population (Sherman et al., 2016). The current preclinical mechanistic studies complement current ongoing clinical testing of sub-anesthetic ketamine for the treatment of LID by our group. Given its clinically proven therapeutic benefit for both treatment-resistant depression (Andrade, 2017) and several pain states (Niesters et al., 2014), very common co-morbidities in PD (Eskow Jaunarajs et al., 2011; Jankovic, 2005), sub-anesthetic ketamine could provide a multifaceted benefit to individuals with PD in the future.

Supplementary Material

Refer to Web version on PubMed Central for supplementary material.

Acknowledgements

This works was supported by the Jerry T. and Glenda G. Jackson Fellowship in Parkinson's Research to the University of Arizona (SJS, TF), the Evelyn F. McKnight Brain Institute (SLC), the Arizona Biomedical Research Commission [ADHS18–198846, SJS, TF], and the National Institute of Health [NIH R56-NS109608, TF; NIH T35-HL007479, MJB]. MJB would like to thank the Society for Neuroscience's Neuroscience Scholars Program for his Fellowship and AJF the ARCS Foundation for his Scholar award.

References

Akinfiresoye L, Tizabi Y, 2013. Antidepressant effects of AMPA and ketamine combination: role of hippocampal BDNF, synapsin, and mTOR. Psychopharmacology 230, 291–298. [PubMed: 23732839]

Alamian G, Hincapié AS, Combrisson E, Thiery T, Martel V, Althukov D, Jerbi K, 2017. Alterations of intrinsic brain connectivity patterns in depression and bipolar disorders: a critical assessment of magnetoencephalography-based evidence. Front. Psych. 8, 41.

Alonso M, Medina JH, Pozzo-Miller L, 2004. ERK1/2 activation is necessary for BDNF to increase dendritic spine density in hippocampal CA1 pyramidal neurons. Learn. Mem. 11, 172–178. [PubMed: 15054132]

Altar CA, Cai N, Bliven T, Juhasz M, Conner JM, Acheson AL, Lindsay RM, Wiegand SJ, 1997. Anterograde transport of brain-derived neurotrophic factor and its role in the brain. Nature 389, 856–880. [PubMed: 9349818]

Andrade C, 2017. Ketamine for depression, 1: clinical summary of issues related to efficacy, adverse effects, and mechanism of action. J. Clin. Psychiatry 78, e415–e419. [PubMed: 28448702]

Autry AE, Adachi M, Nosyreva E, Na ES, Los MF, Cheng P, Kavalali ET, Monteggia LM, 2011. NMDA receptor blockade at rest triggers rapid behavioural antidepressant responses. Nature 475, 91–95. [PubMed: 21677641]

Bartlett MJ, Joseph RM, LePoidevin LM, Parent KL, Laude ND, Lazarus LB, Heien ML, Estevez M, Sherman SJ, Falk T, 2016. Long-term effect of sub-anesthetic ketamine in reducing L-DOPA-induced dyskinesias in a preclinical model. Neurosci. Lett. 612, 121–125. [PubMed: 26644333]

Belujon P, Lodge DJ, Grace AA, 2010. Aberrant striatal plasticity is specifically associated with dyskinesia following levodopa treatment. Mov. Disord. 25, 1568–1576. [PubMed: 20623773]

Bosch M, Hayashi Y, 2012. Structural plasticity of dendritic spines. Curr. Opin. Neurobiol. 22, 383–388. [PubMed: 21963169]

Boulle F, Kenis G, Cazorla M, Hamon M, Steinbusch HWM, Lanfumey L, van den Hove DLA, 2012. TrkB inhibition as a therapeutic target for CNS-related disorders. Prog. Neurobiol. 98 (2), 197–206. [PubMed: 22705453]

Bramham CR, Messaoudi E, 2005. BDNF function in adult synaptic plasticity: the synaptic consolidation hypothesis. Prog. Neurobiol. 76, 99–125. [PubMed: 16099088]

Bresink I, Danysz W, Parsons CG, Mutschler E, 1995. Different binding affinities of NMDA receptor channel blockers in various brain regions—indication of NMDA receptor heterogeneity. Neuropharmacology 34, 533–540. [PubMed: 7566488]

Castrén E, Antila H, 2017. Neuronal plasticity and neurotrophic factors in drug responses. Mol. Psychiatry 22, 1085–1095. [PubMed: 28397840]

Cazorla M, Prémont J, Mann A, Girard N, Kellendonk C, Rognan D, 2011. Identification of a low–molecular weight TrkB antagonist with anxiolytic and antidepressant activity in mice. J. Clin. Invest. 121, 1846–1857. [PubMed: 21505263]

Cenci MA, Crossman AR, 2018. Animal models of l-dopa-induced dyskinesia in Parkinson's disease. Mov. Disord. 33 (6), 889–899. [PubMed: 29488257]

Decressac M, Björklund A, 2013. mTOR inhibition alleviates L-DOPA-induced dyskinesia in parkinsonian rats. J. Parkinsons Dis. 3 (1), 13–17. [PubMed: 23938307]

Dekundy A, Lundblad M, Danysz W, Cenci MA, 2007. Modulation of L-DOPA-induced abnormal involuntary movements by clinically tested compounds: further validation of the rat dyskinesia model. Behav. Brain Res. 179 (1), 76–89. [PubMed: 17306893]

Ding Y, Won L, Britt JP, Lim SA, McGehee DS, Kang UJ, 2011. Enhanced striatal cholinergic neuronal activity mediates L-DOPA-induced dyskinesia in parkinsonian mice. Proc. Natl. Acad. Sci. U. S. A. 108 (2), 840–845. [PubMed: 21187382]

Dunkley BT, Doesburg SM, Sedge PA, Grodecki RJ, Shek PN, Pang EW, Taylor MJ, 2014. Resting-state hippocampal connectivity correlates with symptom severity in post-traumatic stress disorder. Neuroimage Clin. 5, 377–384. [PubMed: 25180157]

Eskow Jaunarajs KL, Angoa-Perez M, Kuhn DM, Bishop C, 2011. Potential mechanisms underlying anxiety and depression in Parkinson's disease: consequences of l-DOPA treatment. Neurosci. Biobehav. Rev. 35 (3), 556–564. [PubMed: 20615430]

Feder A, Parides MK, Murrough JW, Perez AM, Morgan JE, Saxena S, Kirkwood K, Aan Het Rot M, Lapidus KA, Wan LB, Iosifescu D, Charney DS, 2014. Efficacy of intravenous ketamine for treatment of chronic posttraumatic stress disorder: a randomized clinical trial. JAMA Psychiat. 76, 681–688.

Finck AD, Ngai SH, 1982. Opiate receptor mediation of ketamine analgesia. Anesthesiology 56, 291–297. [PubMed: 6278991]

Fischer D, Kemp CJ, Cole-Strauss A, Polinski NK, Paumier KL, Lipton JW, Steece-Collier K, Collier TJ, Buhlinger DJ, Sortwell CE, 2017. Subthalamic nucleus deep brain stimulation employs trkB signaling for neuroprotection and functional restoration. J. Neurosci. 37, 6786–6796. [PubMed: 28607168]

Flores AJ, Bartlett MJ, So LY, Laude ND, Parent KL, Heien ML, Sherman SJ, Falk T, 2014. Differential effects of the NMDA receptor antagonist MK-801 on dopamine receptor D1- and

D2-induced abnormal involuntary movements in a preclinical model. Neurosci. Lett. 564, 48–52. [PubMed: 24525249]

Flores AJ, Bartlett MJ, Root BK, Parent KL, Heien ML, Porreca F, Polt R, Sherman SJ, Falk T, 2018. The combination of the opioid glycopeptide MMP-2200 and a NMDA receptor antagonist reduced L-DOPA-induced dyskinesia and MMP-2200 by itself reduced dopamine receptor 2-like agonist-induced dyskinesia. Neuropharmacology 141, 260–271. [PubMed: 30201210]

Fox SH, Lang AE, Brotchie JM, 2006. Translation of nondopaminergic treatments for levodopa-induced dyskinesia from MPTP-lesioned nonhuman primates to phase IIa clinical studies: keys to success and roads to failure. Mov. Disord. 21, 1578–1594. [PubMed: 16874752]

Gonul SA, Akdeniz F, Taneli F, Donat O, Eker Ç, Vahip S, 2005. Effect of treatment on serum brain–derived neurotrophic factor levels in depressed patients. Eur. Arch. Psychiatry Clin. Neurosci. 255, 381–386. [PubMed: 15809771]

Gu D, Huang J, Yin Y, Shan Z, Zheng S, Wu P, 2014. Long-term ketamine abuse induces cystitis in rats by impairing the bladder epithelial barrier. Mol. Biol. Rep. 41, 7313–7322. [PubMed: 25091940]

Guillin O, Diaz J, Carroll P, Griffon N, Schwartz JC, Sokoloff P, 2001. BDNF controls dopamine D3 receptor expression and triggers behavioural sensitization. Nature 411 (6833), 86–89. [PubMed: 11333982]

Harraz MM, Tyagi R, Cortés P, Snyder SH, 2016. Antidepressant action of ketamine via mTOR is mediated by inhibition of nitrergic rheb degradation. Mol. Psychiatry 21, 313–319. [PubMed: 26782056]

Hashimoto K, 2020. Brain-derived neurotrophic factor-TrkB signaling and the mechanism of antidepressant activity by ketamine in mood disorders. Eur. Arch. Psychiatry Clin. Neurosci. 270, 137–138. [PubMed: 32008067]

Herz DM, Haagensen BN, Christensen MS, Madsen KH, Rowe JB, Løkkegaard A, Siebner HR, 2015. Abnormal dopaminergic modulation of striato-cortical networks underlies levodopa-induced dyskinesias in humans. Brain 138, 1658–1666. [PubMed: 25882651]

Huot P, Johnston TH, Koprich JB, Fox SH, Brotchie JM, 2013. The pharmacology of L-DOPA-induced dyskinesia in Parkinson's disease. Pharmacol. Rev. 65, 171–222. [PubMed: 23319549]

Jankovic J, 2005. Motor fluctuations and dyskinesias in Parkinson's disease: clinical manifestations. Mov. Disord. 20, S11–S16.

Jenkinson N, Brown P, 2011. New insights into the relationship between dopamine, beta oscillations and motor function. Trends Neurosci. 34, 611–618. [PubMed: 22018805]

Kaufman MB, 2019. Pharmaceutical approval update PT. 44, 251–254.

Kneynsberg A, Collier TJ, Manfredsson FP, Kanaan NM, 2016. Quantitative and semi-quantitative measurements of axonal degeneration in tissue and primary neuron cultures. J. Neurosci. Methods 266, 32–41. [PubMed: 27031947]

Levine ND, Rademacher DJ, Collier TJ, O'Malley JA, Kells AP, San Sebastian W, Bankiewicz KS, Steece-Collier K, 2013. Advances in thin tissue Golgi-cox impregnation: fast, reliable methods for multi-assay analyses in rodent and non-human primate brain. J. Neurosci. Methods 213, 214–227. [PubMed: 23313849]

Li L, Vlisides PE, 2016. Ketamine: 50 years of modulating the mind. Front. Hum. Neurosci. 10, 612. [PubMed: 27965560]

Li N, Lee B, Liu RJ, Banasr M, Dwyer JM, Iwata M, Li XY, Aghajanian G, Duman RS, 2010. mTOR-dependent synapse formation underlies the rapid antidepressant effects of NMDA antagonists. Science 329, 959–964. [PubMed: 20724638]

Lipton JO, Sahin M, 2014. The neurology of mTOR. Neuron 84, 275–291. [PubMed: 25374355]

Marras C, Turner CM, 2004. Chapter 11. In: Watts RL, Koller WC (Eds.), Movement Disorders, Neurological Principles and Practice, Second edition. The Macgraw-Hill Companies, Inc..

Miller OH, Moran JT, Hall BJ, 2016. Two cellular hypotheses explaining the initiation of ketamine's antidepressant actions: direct inhibition and disinhibition. Neuropharmacology 100, 17–26. [PubMed: 26211972]

Monteggia LM, Luikart B, Barrot M, Theobold D, Malkovska I, Nef S, Parada LF, Nestler EJ, 2007. Brain-derived neurotrophic factor conditional knockouts show gender differences in depression-related behaviors. Biol. Psychiatry 61, 187–197. [PubMed: 16697351]

Monville C, Torres ET, Dunnett SB, 2006. Comparison of incremental and accelerating protocols of the rotarod test for the assessment of motor deficits in the 6-OHDA model. J. Neurosci. Methods 158 (2), 219–223. [PubMed: 16837051]

Nicolás MJ, López-Azcárate J, Valencia M, Alegre M, Pérez-Alcázar M, Iriarte J, Artieda J, 2011. Ketamine-induced oscillations in the motor circuit of the rat basal ganglia. PLoS One 6 (7), e21814. [PubMed: 21829443]

Niesters M, Martini C, Dahan A, 2014. Ketamine for chronic pain: risks and benefits. Br. J. Clin. Pharmacol. 77, 357–367. [PubMed: 23432384]

Nishijima H, Suzuki S, Kon T, Funamizu Y, Ueno T, Haga R, Suzuki C, Arai A, Kimura T, Suzuki C, Meguro R, Miki Y, Yamada J, Migita K, Ichinohe N, Ueno S, Baba M, Tomiyama M, 2014. Morphologic changes of dendritic spines of striatal neurons in the levodopa-induced dyskinesia model. Mov. Disord. 29, 336–343. [PubMed: 24573720]

Olanow CW, Stern MB, Sethi K, 2009. The scientific and clinical basis for the treatment of Parkinson disease. Neurology 72, S1–S136.

Pacheco DF, Romero TR, Duarte ID, 2014. Central antinociception induced by ketamine is mediated by endogenous opioids and μ- and δ-opioid receptors. Brain Res. 1562, 69–75. [PubMed: 24675031]

Paquette MA, Anderson AM, Lewis JR, Meshul CK, Johnson SW, Berger PS, 2010. MK-801 inhibits L-DOPA-induced abnormal involuntary movements only at doses that worsen parkinsonism. Neuropharmacology 58, 1002–1008. [PubMed: 20079362]

Parise EM, Alcantara LF, Warren BL, Wright KN, Hadad R, Sial OK, Kroeck KG, Iñiguez SD, Bolaños-Guzmán CA, 2013. Repeated ketamine exposure induces an enduring resilient phenotype in adolescent and adult rats. Biol. Psychiatry 74 (10), 750–759. [PubMed: 23790225]

Paxinos G, Watson C, 2007. The Rat Brain in Stereotaxic Coordinates, Sixth ed. Academic Press.

Qiao H, Li MX, Xu C, Chen HB, An SC, Ma XM, 2016. Dendritic spines in depression: what we learned from animal models. Neural Plast. 2016, 8056370.

Rascol O, Perez-Lloret S, Ferreira JJ, 2015. New treatments for levodopa-induced motor complications. Mov. Disord. 30 (11), 1451–1460. [PubMed: 26293004]

Reichardt LF, 2006. Neurotrophin-regulated signalling pathways. Philos. Trans. R. Soc. Lond. B Biol. Sci. 361 (1473), 1545–1564. [PubMed: 16939974]

Rogawski MA, 2008. Common pathophysiologic mechanisms in migraine and epilepsy. Arch. Neurol. 65, 709–714. [PubMed: 18541791]

Salazar G, Motamed C, 2012. A remifentanil/ketamine sedation in surgical cancer patients having severe Parkinson's disease: two case reports. J. Opioid Manag. 8, 133–134. [PubMed: 22616319]

Samadi P, Bédard PJ, Rouillard C, 2006. Opioids and motor complications in Parkinson's disease. Trends Pharmacol. Sci. 27, 512–517. [PubMed: 16908075]

Savitt JM, Dawson VL, Dawson TM, 2006. Diagnosis and treatment of Parkinson disease: molecules to medicine. J. Clin. Invest. 116, 1744–1754. [PubMed: 16823471]

Schapira AH, Jenner P, 2011. Etiology and pathogenesis of Parkinson's disease. Mov. Disord. 26, 1049–1055. [PubMed: 21626550]

Sgambato-Faure V, Cenci MA, 2012. Glutamatergic mechanisms in the dyskinesias induced by pharmacological dopamine replacement and deep brain stimulation for the treatment of Parkinson's disease. Prog. Neurobiol. 96 (1), 69–86. [PubMed: 22075179]

Shen W, Flajolet W, Greengard P, Surmeier DJ, 2008. Dichotomous dopaminergic control of striatal synaptic plasticity. Science 321, 848–851. [PubMed: 18687967]

Sherman SJ, Estevez M, Magill AB, Falk T, 2016. Case reports showing a long-term effect of subanesthetic ketamine infusion in reducing L-DOPA-induced dyskinesias. Case Rep. Neurol. 8, 53–58. [PubMed: 27293405]

Shirayama Y, Chen A, Nakagawa S, Russell DS, Duman RS, 2002. Brain-derived neurotrophic factor produces antidepressant effects in behavioral models of depression. J. Neurosci. 22, 3251–3261. [PubMed: 11943826]

Su R, Zhen J, Wang W, Zhang J, Zheng Y, Wang X, 2018. Time-course behavioral features are correlated with Parkinson's disease-associated pathology in a 6-hydroxydopamine hemiparkinsonian rat model. Mol. Med. Rep. 17, 3356–3363. [PubMed: 29257290]

Suarez L, Solis O, Aguado C, Lujan R, Moratalla R, 2016. L-DOPA oppositely regulates synaptic strength and spine morphology in D1 and D2 striatal projection neurons in dyskinesia. Cereb. Cortex 26, 4253–4264. [PubMed: 27613437]

Suppa E, Valente A, Catarci S, Zanfini BA, Draisci G, 2012. A study of low-dose S-ketamine infusion as "preventive" pain treatment for cesarean section with spinal anesthesia: benefits and side effects. Minerva Anestesiol. 78, 774–781. [PubMed: 22374377]

Treccani G, Ardalan M, Chen F, Musazzi L, Popoli M, Wegener G, Nyengaard J, Müller H, 2019. S-Ketamine reverses hippocampal dendritic spine deficits in flinders sensitive line rats within 1 h of administration. Mol. Neurobiol. 56 (11), 7368–7379. [PubMed: 31037646]

Tronci E, Napolitano F, Muñoz A, Fidalgo C, Rossi F, Björklund A, Usiello A, Carta M, 2017. BDNF over-expression induces striatal serotonin fiber sprouting and increases the susceptibility to l-DOPA-induced dyskinesia in 6-OHDA-lesioned rats. Exp. Neurol. 297, 73–81. [PubMed: 28757258]

Welberg L, 2010. Psychiatric disorders: ketamine modifies mood through mTOR. Nat. Rev. Neurosci. 11, 666.

White PF, Schüttler J, Shafer A, Stanski DR, Horai Y, Trevor AJ, 1985. Comparative pharmacology of the ketamine isomers. Studies in volunteers. Br. J. Anaesth. 57, 197–203. [PubMed: 3970799]

Widman AJ, McMahon LL, 2018. Disinhibition of CA1 pyramidal cells by low-dose ketamine and other antagonists with rapid antidepressant efficacy. Proc. Natl. Acad. Sci. U. S. A. 115, E3007–E3016. [PubMed: 29531088]

Williams NR, Heifets BD, Blasey C, Sudheimer K, Pannu J, Pankow H, Hawkins J, Birnbaum J, Lyons DM, Rodriguez CI, Schatzberg AF, 2018. Attenuation of antidepressant effects of ketamine by opioid receptor antagonism. Am. J. Psychiatry 175, 1205–1215. [PubMed: 30153752]

Wright JJ, Goodnight PD, McEvoy MD, 2009. The utility of ketamine for the preoperative management of a patient with Parkinson's disease. Anesth. Analg. 108, 980–982. [PubMed: 19224812]

Yagishita S, Hayashi-Takagi A, Ellis-Davies G, Urakubo H, Ishii S, Kasai H, 2014. A critical time window for dopamine actions on the structural plasticity of dendritic spines. Science 345, 1616–1620. [PubMed: 25258080]

Yang C, Shirayama Y, Zhang J, Ren Q, Yao W, Ma M, Dong C, Hashimoto K, 2015. R-ketamine: a rapid-onset and sustained antidepressant without psychotomimetic side effects. Transl. Psychiatry 5, e632. [PubMed: 26327690]

Ye T, Bartlett MJ, Schmit MB, Sherman SJ, Falk T, Cowen SL, 2018. Ten-hour exposure to low-dose ketamine enhances corticostriatal cross-frequency coupling and hippocampal broad-band gamma oscillations. Front. Neural Circuits 12, 61. [PubMed: 30150926]

Zanos P, Gould T, 2018. Mechanisms of ketamine action as an antidepressant. Mol. Psychiatry 23, 801–811. [PubMed: 29532791]

Zhang Y, Meredith GE, Mendoza-Elias N, Rademacher DJ, Tseng KY, Steece-Collier K, 2013. Aberrant restoration of spines and their synapses in L-DOPA-induced dyskinesia: involvement of corticostriatal but not thalamostriatal synapses. J. Neurosci. 33, 11655–11667. [PubMed: 23843533]

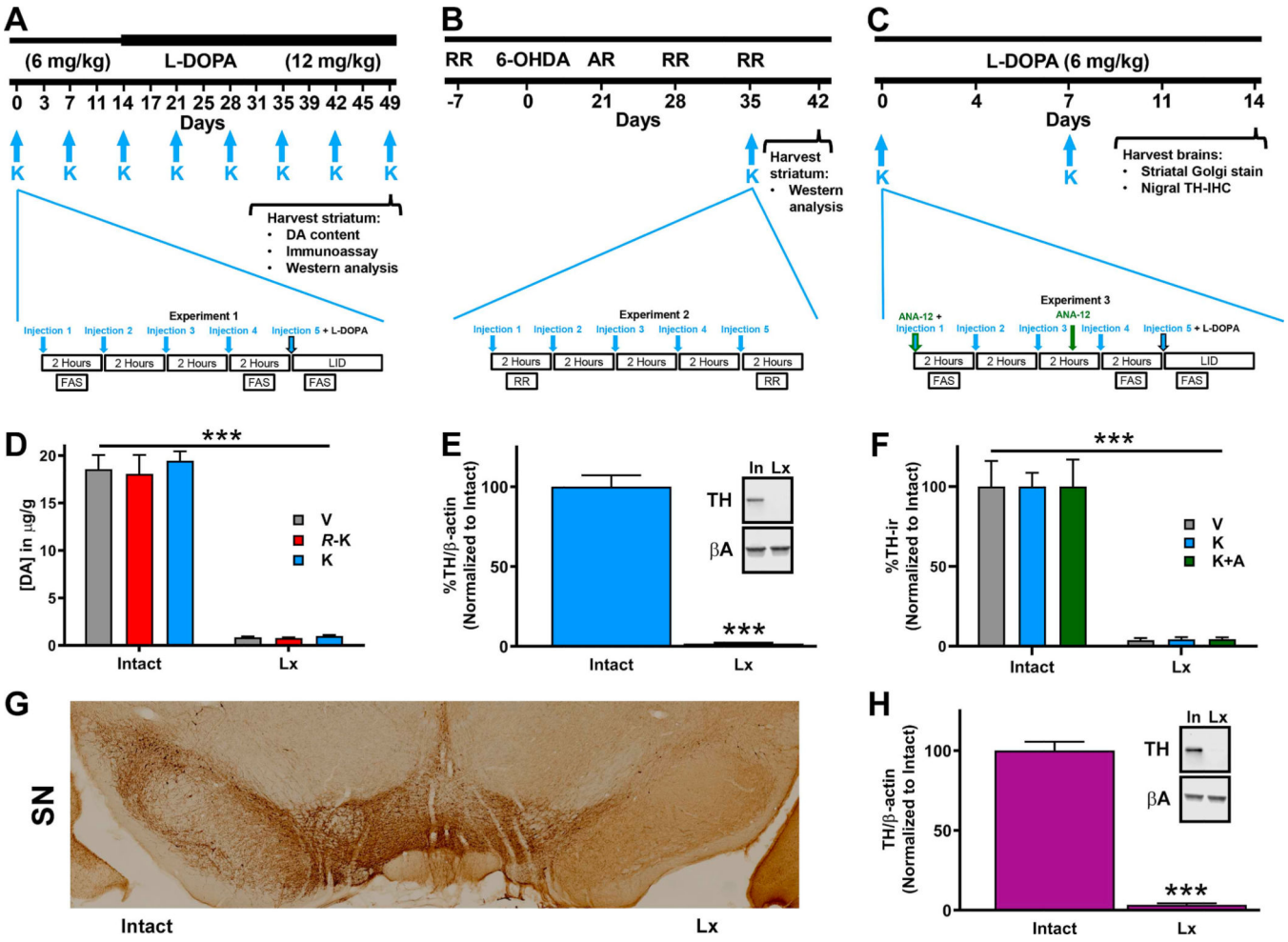

Fig. 1.

Schemes for *Experiments* and *post hoc* analyses. (A) Scheme of the ketamine injection paradigm for *Experiment 1* during development of LID (daily L-DOPA injections). FAS = Forelimb adjusting steps test. (B) Scheme of the injection paradigm in PD rats for *Experiment 2*. AR = amphetamine-rotation test; RR = RotaRod test. (C) Scheme of the injection paradigm for *Experiment 3* during development of LID (daily L-DOPA injections). (D) Verification of unilateral 6-OHDA lesion and evaluation of striatal dopamine (DA) levels after ketamine in the rats from the study shown in (A). Electrochemical detection of striatal DA content (mean ± SEM) is reduced by>95% in the lesioned side. Striatal DA content was unchanged by a 10-h-treatment of either ketamine (K; n=9), *R*-ketamine (*R*-K; n=9) *vs.* vehicle (V; n = 9) 1-h before rats were euthanized, showing no effect on overall striatal DA levels by ketamine or *R*-ketamine-treatment compared to vehicle in either the lesioned (Lx) or the intact hemisphere. (E) Verification of unilateral 6-OHDA lesion from the study shown in (B) using semi-quantitative TH western analysis in striatal tissue plotting % loss (mean ± SEM) in Lx *vs.* intact (In) hemisphere (n=9). Two-tailed t-test, ***$p < .001$. (F) Verification of unilateral 6-OHDA lesions in the rats from the study depicted in (C). The graph shows the quantification of the TH-ir plotting the % loss (mean ± SEM) in the Lx *vs.* intact SN hemispheres (n =10/group; V =vehicle, K =ketamine, K +A = ketamine+ ANA-12). (G)

Example photomicrograph of a SN in *Experiment 3* shows the unilateral reduction in TH-ir post-lesion. Two-way ANOVAs, Bonferroni *post hoc* tests, ***$p < .001$. (H) Verification of unilateral 6-OHDA lesion from the ANA-12-only control study, the negative control for *Experiment 3*, using semi-quantitative TH western analysis in striatal tissue, plotting % loss (mean ± SEM) in Lx *vs.* intact hemisphere ($n = 10$). Two-tailed *t*-test, ***$p < .001$.

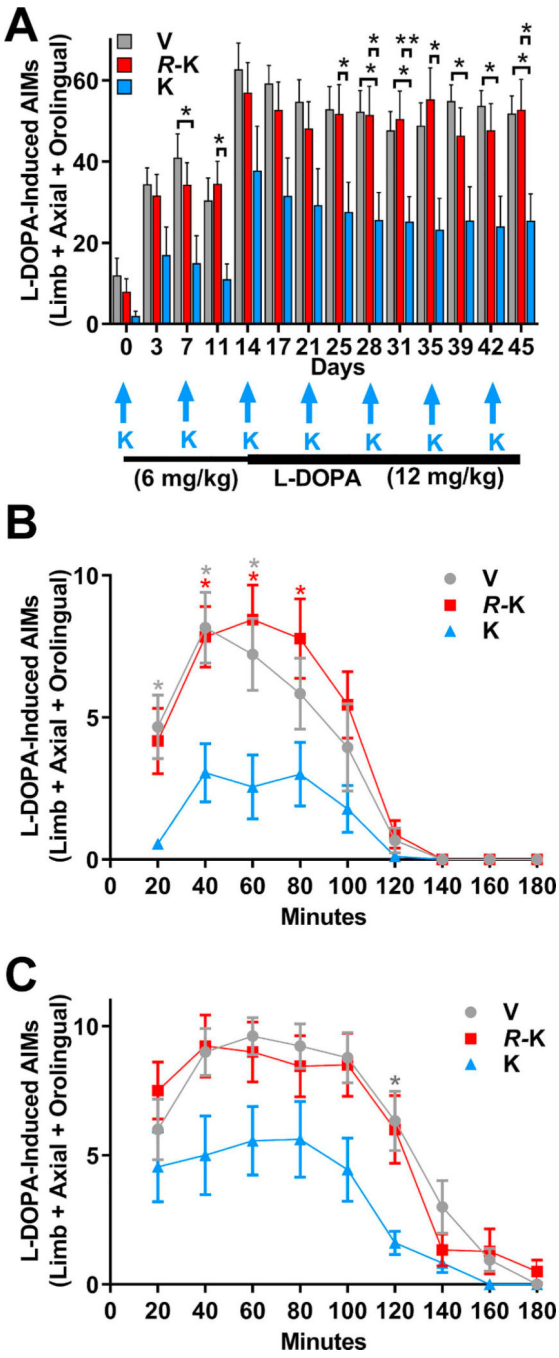

Fig. 2.

Low-dose racemic ketamine treatment once a week attenuates the development of LID in the preclinical model. In *Experiment 1* 6-OHDA-lesioned PD rats were injected daily with L-DOPA (days 0–13: 6 mg/kg; days 14–28: 12 mg/kg; *i.p.*) to induce dyskinesia and tested for LAO-AIMs twice a week for 3 h by blinded investigators. (A) The mean LAO AIMs scores±SEM are plotted showing a 50% reduction after racemic low-dose ketamine treatments (K) when compared to the vehicle group (V) and a group treated with *R*-ketamine (*R*-K), to test for contribution of the stereospecific ketamine isomer. The blue arrows point

to the days of the 10-h racemic ketamine (20 mg/kg; *i.p.*), *R*-ketamine (10 mg/kg; *i.p.*) or vehicle treatment paradigm; $n = 9$ per group, $*p < .05$, $**p < .01$, Kruskal-Wallis test with Dunn's multiple comparisons *post hoc* tests. (B) Example time course of the LAO-AIMs data showed in (A) for day 11. (C) Example time course of the LAO-AIMs data showed in (A) for day 25. (For interpretation of the references to colour in this figure legend, the reader is referred to the web version of this article.)

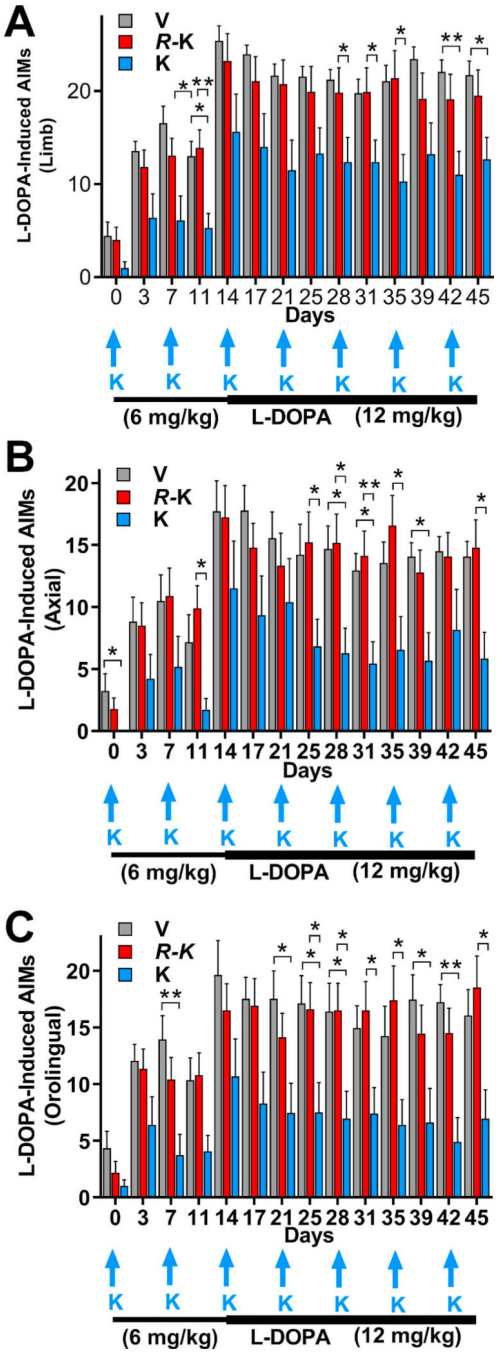

Fig. 3.

LAO-AIMs scores from *Experiment 1* separated by sub-type of dyskinesia. Low-dose racemic ketamine treatment once a week attenuates the development of (A) limb (B) axial (C) orolingual AIMs in the preclinical model. 6-OHDA-lesioned PD rats were injected daily with L-DOPA (days 0–13: 6 mg/kg; days 14–28: 12 mg/kg; *i.p.*) to induce dyskinesia and tested for LAO AIMs twice a week for 3 h by blinded investigators. The mean LAO AIMs scores ± SEM are plotted showing a 50% reduction after racemic low-dose ketamine treatments (K) when compared to the vehicle group (V) and a group treated with *R*-ketamine

(*R*-K), to test for contribution of the stereospecific ketamine isomer. The blue arrows point to the days of the 10-h racemic ketamine (20 mg/kg; *i.p.*), *R*-ketamine (10 mg/kg; *i.p.*) or vehicle treatment paradigm; $n = 9$ per group, $*p < .05$, $**p < .01$, Kruskal-Wallis tests with Dunn's *post hoc* tests. (For interpretation of the references to colour in this figure legend, the reader is referred to the web version of this article.)

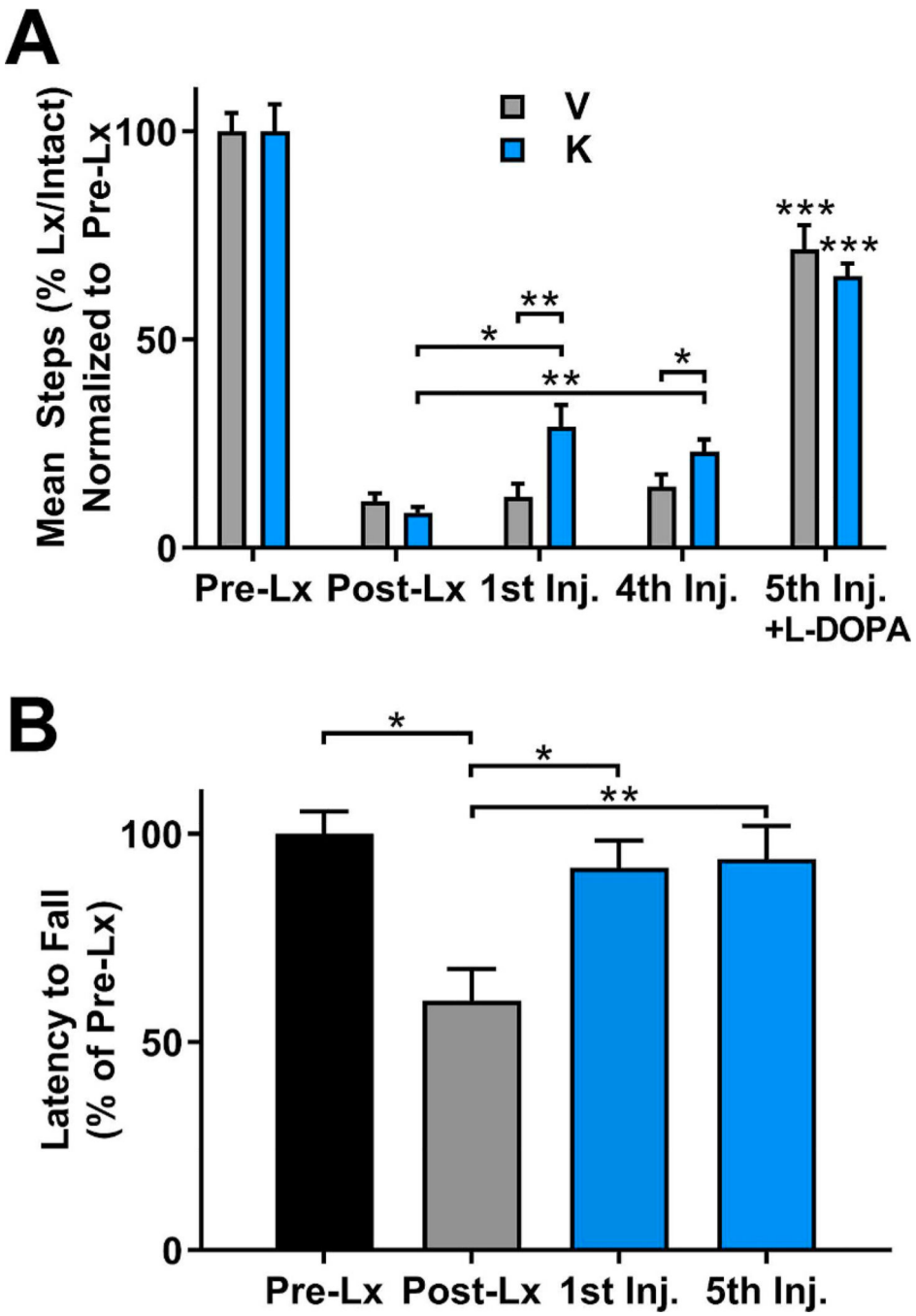

Fig. 4.

Ketamine does not interfere with the anti-PD effect of L-DOPA and reduces PD-motor behavior post-6-OHDA-lesion (Post-Lx) by itself. (A) Mean % contralateral/ipsilateral ratios of steps ± SEM using the FAS test paradigm in the LID cohort of *Experiment 1*, are plotted after normalization to pre-lesion (Pre-Lx) indicate a significant anti-PD effect of ketamine *$p < .05$; repeated measures ANOVA. Ketamine does also not interfere with the anti-PD effect of L-DOPA, and a significant increase of stepping contralateral to the lesioned side after either L-DOPA alone or L-DOPA + Ketamine *vs.* all Post-Lx time points is seen: ***p

< .001; one-way ANOVA on data prior to normalization, Tukey-Kramer corrected *post hoc* tests; $n = 9$ per group. (B) In *Experiment 2* we tested ketamine treatment in a separate cohort of hemi-parkinsonian 6-OHDA-lesioned rats and used the RotaRod test to evaluate the deficit. The graph shows the mean latency to fall ± SEM, normalized to pre-lesion baseline (Pre-Lx). Post-lesion (Post-Lx) the latency to fall was reduced by 50% in these PD animals. This motor deficit was reversed by ketamine treatment (blue bars), already at the 1st injection, and the animals performed as good as at baseline. One-way ANOVA, with Tukey-Kramer corrected *post hoc* tests, on raw data before normalization. $n = 9$, $*p < .05$, $**p < .01$. (For interpretation of the references to colour in this figure legend, the reader is referred to the web version of this article.)

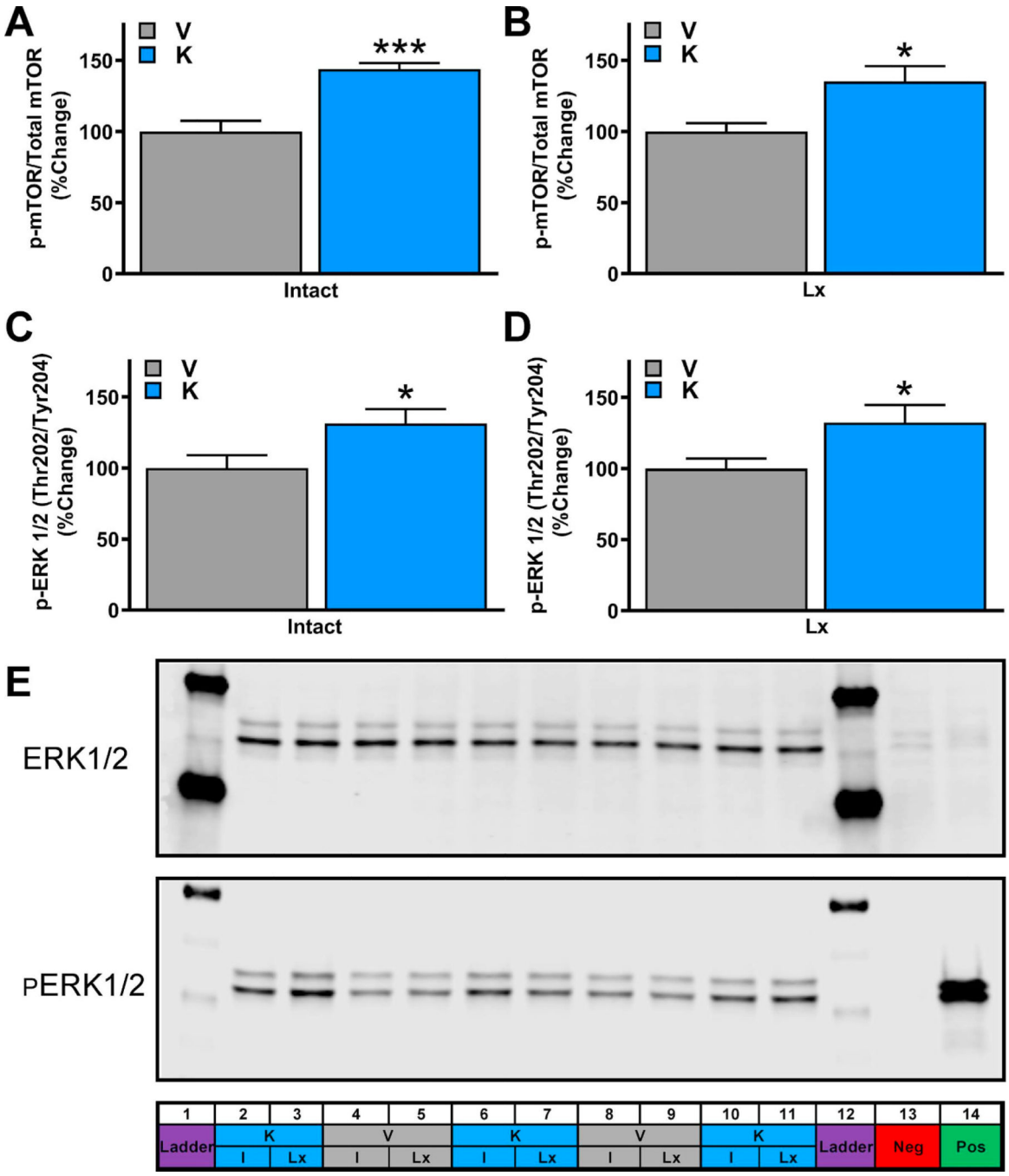

Fig. 5.

Ketamine did activate striatal mTOR and ERK1/2 pathways. (A, B) Involvement of the mTOR pathway in the effects of ketamine. We show an increased phosphorylation level of striatal mTOR in striatal tissue using a multiplex immunoassay. Mean % p-mTOR / mTOR level ± SEM normalized to vehicle control is plotted for the intact (A) and lesioned (B) striatum for vehicle control (V) and ketamine (K) conditions. $n = 9$ per group, $*p < .05$, $***p < .001$; two-tailed t-tests on data prior to normalization. (C, D) Western analysis of levels of striatal ERK1/2 phosphorylation. Mean % p-ERK1/2 / ERK1/2 level ± SEM

normalized to vehicle control is plotted for the intact (C) and lesioned (D) hemispheres. *$p < .05$; two-tailed *t*-tests on data prior to normalization. (E) Example western blots testing for pERK1/2 and total ERK1/2 are shown. I = intact hemisphere; Lx = lesioned hemisphere; Neg = negative control; Pos = positive control.

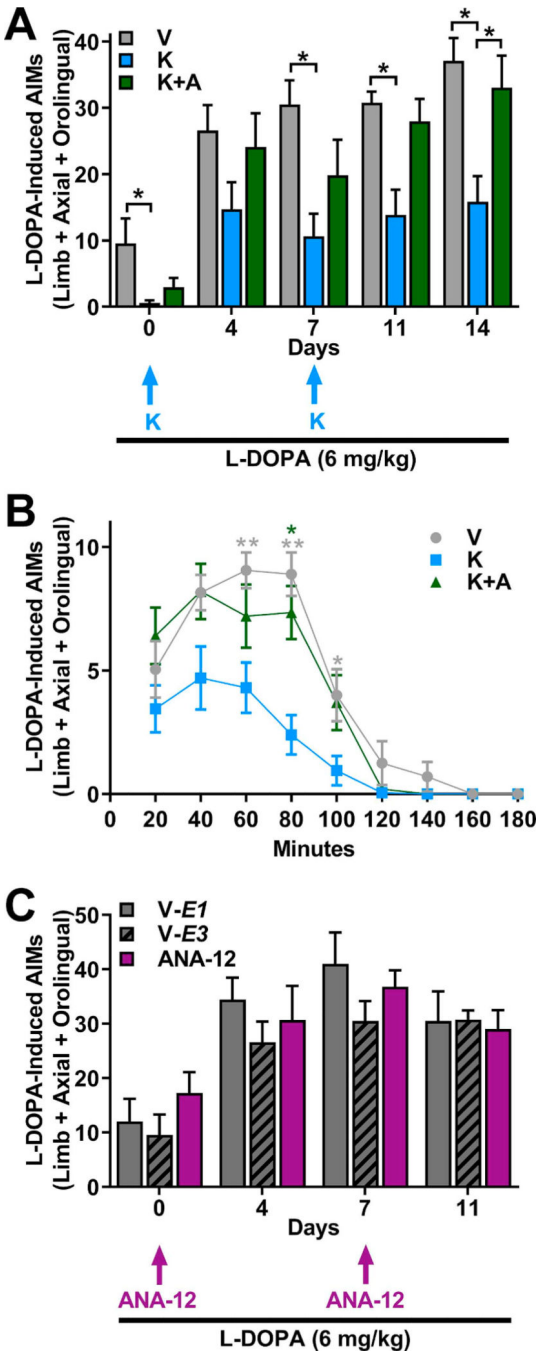

Fig. 6.

Ketamine's long-term anti-dyskinetic activity was driven by BDNF signaling. (A) The mean LAO-AIMs scores ± SEM of *Experiment 3* are plotted. The sustained anti-dyskinetic effect of low-dose ketamine is reduced by blocking the BDNF receptor TrkB, with co-injection of the TrkB antagonist ANA-12 (0.5 mg/kg; *i.p.*) with ketamine (K + A). The blue arrows point to the days of the 10-h racemic (K) ketamine (20 mg/kg; *i.p.*), or vehicle treatment paradigm (V). ANA-12 co-injection (green bars) did reduce the sustained anti-dyskinetic effect seen in ketamine-only injected LID (blue bars) leading to LAO AIMs comparable to

those of the vehicle group (grey bars), indicating an involvement of BDNF in the sustained anti-dyskinetic effects of ketamine. $n = 10$ per group, $*p < .05$, $**p < .01$, ANOVAs, Tukey-Kramer corrected *post hoc* tests. (B) Example time course of the LAO-AIMs for day 14 showed in (A). (C) A control study using 10-h ANA-12-only treatments on days 0 and 7 of daily L-DOPA-treatment (6 mg/kg; *i.p.*) verified that, while systemic TrkB antagonism does block the ketamine effect, it does not change development of LID in this model, and serves as an important negative control for the data shown in (A). The graph depicts the mean LAO-AIMs scores ± SEM from the vehicle control groups in *Experiment 1* (V-*E1*; $n = 9$) and *Experiment 3* (V-*E3*; $n = 10$), as well as the ANA-12-only control study (ANA-12; $n = 10$). (For interpretation of the references to colour in this figure legend, the reader is referred to the web version of this article.)

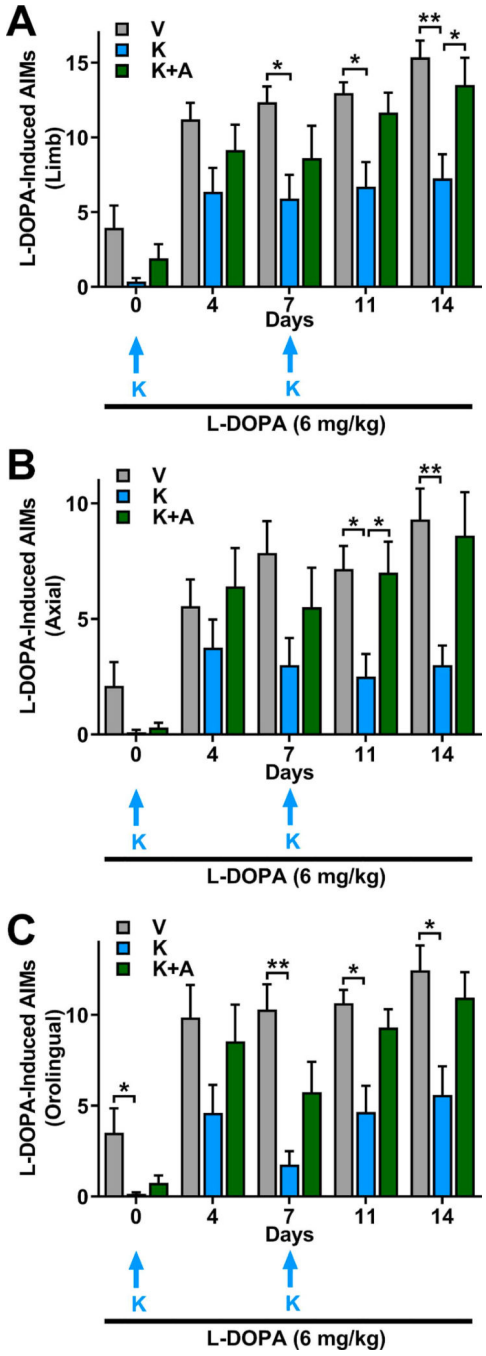

Fig. 7.

LAO-AIMs scores from *Experiment 3* separated by sub-type of dyskinesia. Low-dose ketamine treatment (blue arrows) once a week attenuates the development of individual AIMs scores. 6-OHDA-lesioned PD rats were injected daily with L-DOPA (days 0–14: 6 mg/kg; *i.p.*) to induce dyskinesia and tested for LAO-AIMs twice a week for 3 h by blinded investigators. The anti-dyskinetic effect of low-dose ketamine (K, blue bars) reduced the individual (A) limb (B) axial (C) and orolingual AIMs (mean ± SEM) scores, compared to the vehicle (V, grey bars) group and a group treated with the TrkB antagonist, ANA-12 (K +

A, green bars). The blue arrows point to the days of the 10-h racemic ketamine (20 mg/kg; *i.p.*), *R*-ketamine (10 mg/kg; *i.p.*) $n = 10$ per group, $*p < .05$, $**p < .01$, Kruskal-Wallis tests with Dunn's *post hoc* tests. (For interpretation of the references to colour in this figure legend, the reader is referred to the web version of this article.)

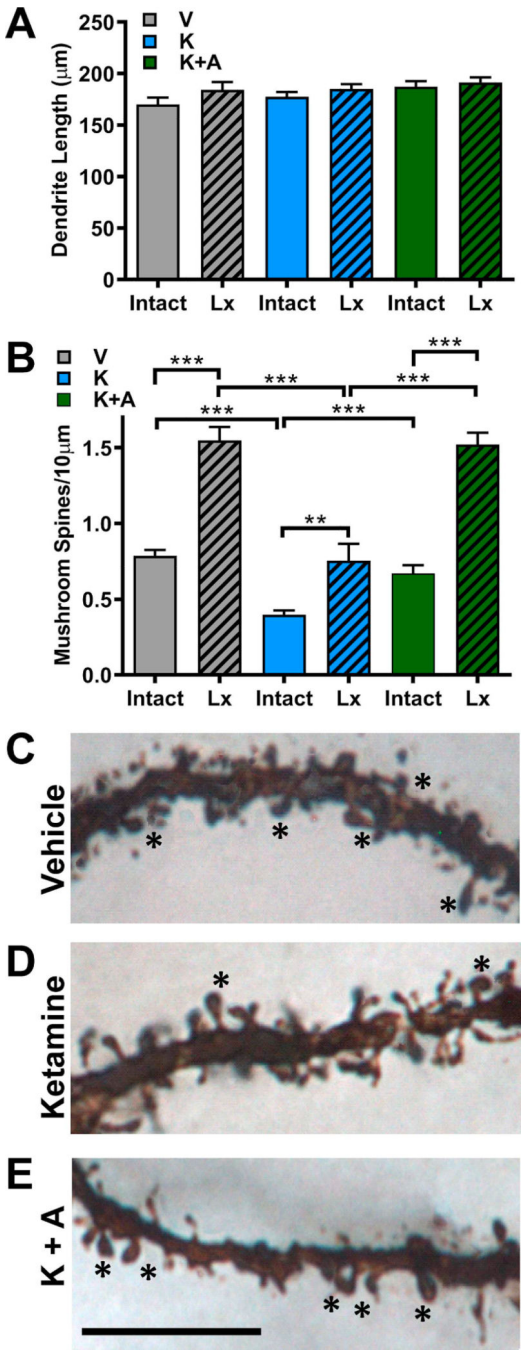

Fig. 8.

Ketamine reduced dendritic mushroom spines in the dyskinetic striatum. (A) The mean dendritic length of the MSN neurons (± SEM) is plotted for intact and lesioned hemisphere for all the treatment groups. No significant difference was found between groups for dendritic length. (B) Ketamine-treated rats (K) showed a significant reduction of mushroom spine density in medium spiny neurons (MSNs) of the dorsal striatum in both the intact and lesioned hemispheres, as compared to vehicle controls (V). Mushroom spines were at control levels in rats co-treated with ketamine and the TrkB receptor antagonist, ANA-12

(K + A). Example photomicrographs of lesioned hemispheres with * indicating mushroom spines are shown for vehicle treatment (C), ketamine treatment (D), and co-treatment with ketamine and ANA-12 (E). Scale bar = 10 μm. $n = 10$ rats/group, and $n = 3$ dendrites/hemisphere, $^{**}p < .01$, $^{***}p < .001$. One-way ANOVA with Sidak's multiple comparisons test.

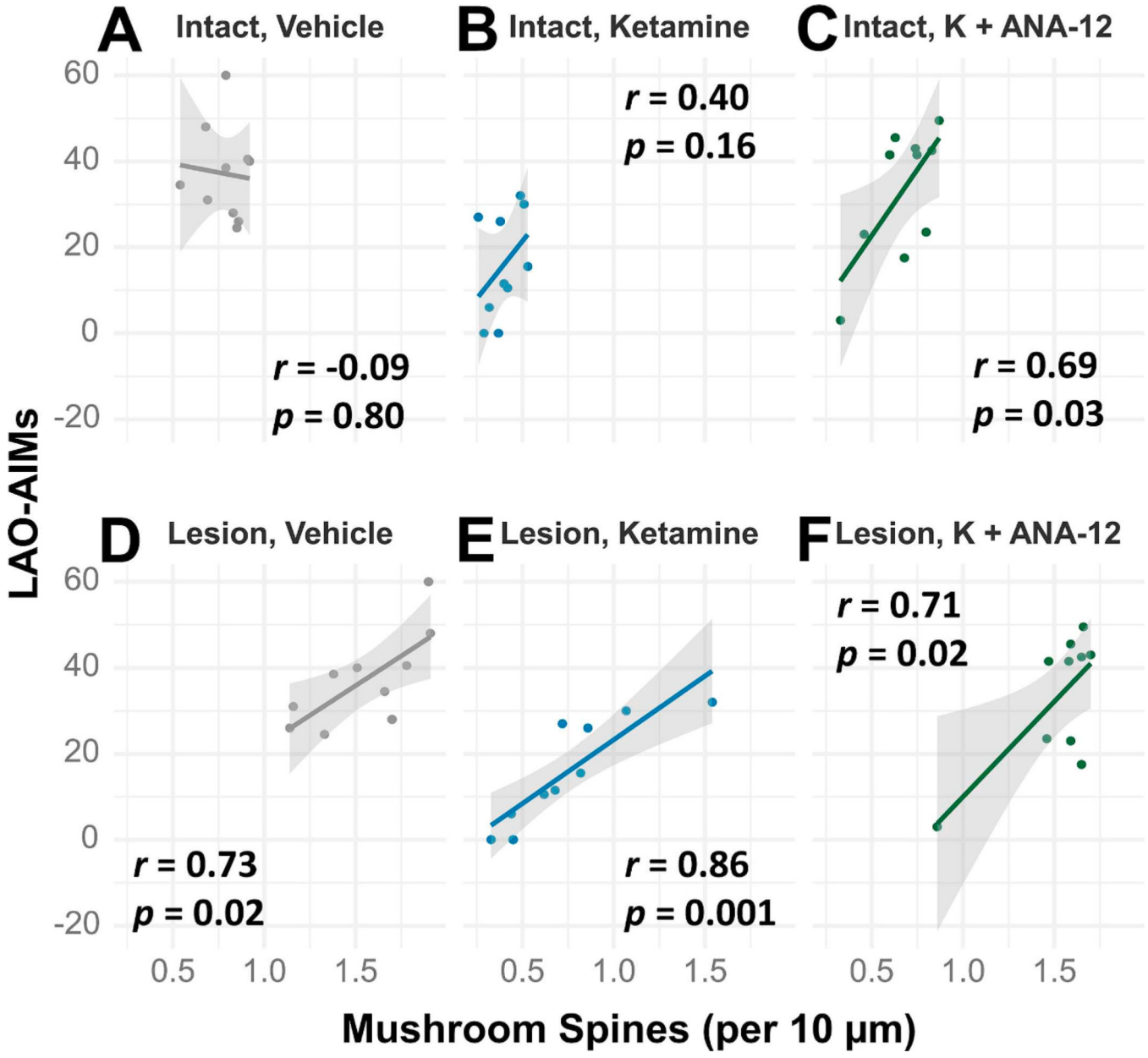

Fig. 9.

LAO-AIMs are correlated with mushroom spines in the lesioned dyskinetic striatum. Correlation analyses of mushroom spine density (mean ± SEM) as compared to total LAO-AIMs (mean ± SEM) are shown for (A) vehicle, intact, (B) ketamine, intact hemisphere, (C) ketamine + ANA-12, intact hemisphere, (D) vehicle, lesioned hemisphere, (E) ketamine, lesioned hemisphere, (F) and ketamine + ANA-12, lesioned hemisphere. There was a high correlation between mushroom spines and LAO-AIMs in the lesioned hemispheres of all treatment groups, indicating the importance of striatal mushroom spine density for LID. n = 10 rats/group, and n = 3 dendrites/hemisphere, Pearson's correlation test.

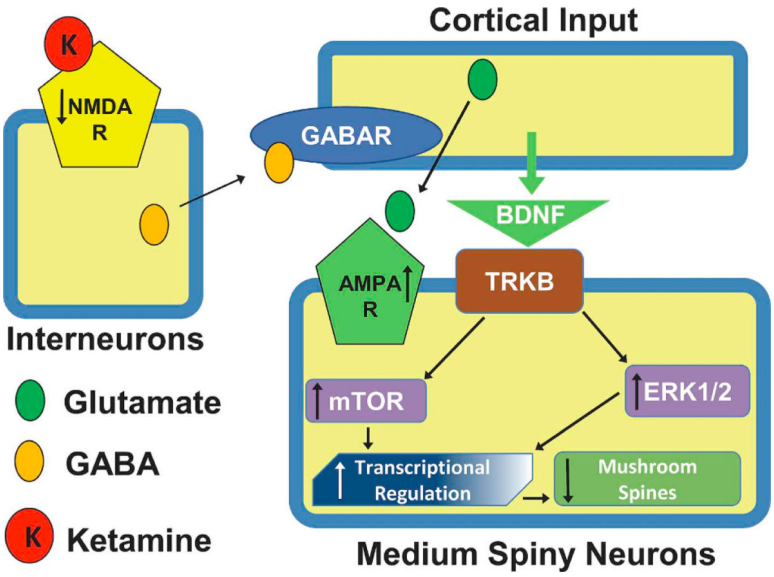

Fig. 10.

Schematic for the proposed molecular mechanisms for the prolonged anti-dyskinetic effects of ketamine. *Cortical disinhibition hypothesis*: Ketamine (K) causes a burst of glutamate thought to occur *via* cortical parvalbumin (PV)-positive gamma-aminobutyric acid (GABA)-interneurons in the motor cortex; the tonic firing of the interneuron is driven by NMDAR*s*, and the active, open-channel state allows ketamine to enter and block activity. The release of inhibition activates glutamatergic principal cells, stimulates α-amino-113-hydroxy-5-methyl-4-isoxazolepropionic acid receptors (AMPARs) and depolarizes downstream striatal MSN neurons. In addition, release of cortical BDNF leads to stimulation of TrkB on striatal MSNs, activating mTOR and ERK1/2, followed by an increase in transcriptional regulation and as a result maladaptive multisynaptic mushroom spines in the dyskinetic striatum are replaced by monosynaptic thin spines.

Table 1

List of Abbreviations.

Abbreviation	Full name
6-OHDA	6-hydroxydopamine
ABC	Avidin-Biotin Complex
AIMs	Abnormal involuntary movements
AMPARs	α-amino-3-hydroxy-5-methyl-4-isoxazolepropionic acid receptors
ANA-12	N-[2-[(2-oxoazepan-3-yl)carbamoyl]phenyl]-1-benzothiophene-2-carboxamide
ANOVA	Analysis of variance
AR	Amphetamine-induced rotation test
ARRIVE	Animal Research: Reporting *In Vivo* Experiments guideline
BDNF	Brain-derived neurotrophic factor
BG	Basal ganglia
D1R	Dopamine 1 receptor
DA	Dopamine
DMSO	Dimethyl sulfoxide
ERK1/2	Extracellular signal-regulated kinases 1/2; also referred to as MAPK
FAS test	Forelimb adjusting steps test
FDA	Food & Drug Administration
GABA	Gamma-aminobutyric acid
HPLC-EC	High-performance liquid chromatography with electrochemical detection
IgG	Immunoglobulin G
IHC	Immunohistochemistry
i.p.	Intraperitoneal
LAO	Limb, Axial and Orolingual
L-DOPA	l-3,4-dihydroxyphenylalanine or levodopa
LID	L-DOPA-induced dyskinesia
MFB	Medial forebrain bundle
MK-801	*N*-methyl-D-aspartate receptor antagonist
MMP-2200	Mixed μ/δ-opioid receptor agonist
MSN	Medium spiny neurons
mTOR	Mammalian target of rapamycin
NMDAR	*N*-methyl-D-aspartate receptor
PD	Parkinson's disease
PFC	Prefrontal cortex
PTSD	Posttraumatic stress disorder
PV	Parvalbumin
RPM	Rotations per minute
RR	RotaRod test
RT	Room temperature
SEM	Standard error of the mean
SN	Substantia nigra pars compacta

Abbreviation	Full name
TH	Tyrosine hydroxylase
TH-ir	TH-immunoreactive
TrkB	Tropomyosin receptor kinase B

Table 2

Histopathological analysis of bladder tissue – no change after ketamine treatment. Table reporting severity of pathology in bladders of treated animals. No differences was seen between vehicle- and ketamine-treatment groups. Categories: 0) no significant lesions, 1) mild segmental submucosal fibrosis, 2) mild segmental submucosal fibrosis with minimal to mild focal non-suppurative cystitis, 3) mild segmental submucosal fibrosis with moderate focal non-suppurative cystitis, 4) mild segmental submucosal fibrosis with severe focal non-suppurative cystitis, 5) moderate segmental submucosal fibrosis, 6) severe segmental submucosal fibrosis.

	Vehicle	Ketamine	Rat #
Pathology Score	0	0	Rat 1
	0	2	Rat 2
	0	2	Rat 3
	1	0	Rat 4
	1	0	Rat 5
	0	0	Rat 6
	1	0	Rat 7
	0	0	Rat 8
	2	1	Rat 9
	2	2	Rat 10
Mean	0.70	0.70	
SEM	0.26	0.30	

Table 3

Correlations between mean LAO-AIMs, and striatal mushroom and thin spines.

		Mean			*r*-value			*p*-value		
		LAO-AIMs	**Mushroom spines**	**Thin spines**	**Mushroom spines vs. LAO**	**Thin spines vs. LAO**	**Mushroom vs. thin spines**	**Mushroom spines vs. LAO**	**Thin spines vs. LAO**	**Mushroom vs. thin spines**
Intact	Vehicle	37.1	0.79	9.5	−0.09	0.25	−0.0063	0.80	0.48	0.99
	Ketamine	15.85	0.40	14.75	0.40	−0.62	−0.13	0.25	0.06	0.72
	K + ANA-12	33.05	0.67	10.44	0.69	0.11	0.19	0.03	0.76	0.60
Lesion	Vehicle	37.1	1.55	8.78	0.72	−0.18	−0.20	0.02	0.61	0.59
	Ketamine	15.85	0.75	14.05	0.86	−0.60	−0.55	0.001	0.06	0.1
	K + ANA-12	33.05	1.52	8.04	0.71	−0.51	−0.30	0.02	0.14	0.39